Final Project Report

Collaborative Research between the University of Kentucky and the University of Memphis:
High–resolution P- and S-wave Velocity Structure of the Post-Paleozoic
Sediments in the Upper Mississippi Embayment

Award Number:
G09AP00096 (University of Memphis)
G09AP000126(University of Kentucky)

Project Duration:
07/01/2009-12/31/20111

Principal Investigators:

Jer-Ming Chiu
Center for Earthquake Research and Information
The University of Memphis
jerchiu@memphis.edu

Edward Woolery and Zhenming Wang
Department of Earth and Environmental Sciences
University of Kentucky
woolery@uky.edu
& zmwang@uky.edu

May 31, 2012

Table of Contents

Introduction 2

Background 3

Vp and Vs Models for Sediments in the Upper Mississippi Embayment 6
- **Previous Studies** 6
- **Field Work** 8
- **Interpretation of Seismic Profiles** 9
- **Deeper Vs for Sites of Thick Sediments** 12

Wave Conversion and Site-Specific Amplification from CUSSO Borehole Array 13
- **Background** 13
- **Wave Conversion and Average Vp and Vs of the Sediments** 14
- **Frequency-Dependent Amplification of Incoming Seismic Waves** 15

Average Vs of the Sediments in the Upper Mississippi Embayment from Converted Waves. 16
- **Background** 16
- **Average Vs for the Post-Paleozoic Sediments in the Upper Mississippi Embayment** 18

Imaging of Shallow Crustal Structure in the Southwestern Kentucky by Using Microearthquake Waveforms 21
- **Abstract** 21
- **Introduction** 21
- **Velocity Structure in the Mississippi Embayment** 24
- **Microearthquake Waveforms** 25
- **Pseudo-imaging Profiling** 26
- **Application: CUKY and HICK in Southwestern Kentucky** 26
  - **CUKY** 27
  - **HICK** 29
- **Discussions** 31
- **Conclusions** 32

Summary 33

Data Management 34

Acknowledgements 34

Attachment A – Site Locations for Seismic Profiles FY09-11 35

References 36

Introduction

Under this project support, 17 PASCAL broadband stations are installed from June 2010 to December 2011 at selected sites within the upper Mississippi Embayment in western Kentucky and northwestern Tennessee. Ground motions from noises, local, regional, and teleseismic earthquakes are recorded continuously with 100 samples/sec at these 17 stations. During this project period, seismic profiles using P- and S-wave sources are also conducted at or near all 17 sites to image Vp and Vs structural models for the post-Paleozoic sediments beneath each site. In addition, a few local, regional, and teleseismic earthquakes are recorded at the Central United States Seismological Observatory (CUSSO), recently installed deep borehole stations by the University of Kentucky. The CUSSO consists of a mixed of five strong motion and two broadband seismic stations deployed at various depths from surface to Paleozoic bedrock at 593 m depth near Hickman, Kentucky. In this project report, preliminary results from the analysis of local, regional, and teleseismic earthquake waveforms, Vp and Vs seismic profiles, and seismic waveforms from the borehole stations will be briefly presented.

Very significant frequency dependent attenuation and amplification of vertically and/or laterally propagating seismic waves across the sediments in the Upper Mississippi Embayment have recently been observed from explosions, local, regional, and teleseismic earthquakes (McIntyre et al., 2011; Chiu et al., 2011; Obikili 2011). Such observations became interpretable from the recently available borehole observations in western Kentucky and from the recent improvement in our understanding of Vp and Vs structural models for the sediments in the embayment. In particular, amplitude of the incoming seismic waves from a local or regional earthquake can be amplified 10~15 times from a borehole station in the Paleozoic bedrock to a station on the surface directly above, but only 2~3 times from large teleseismic event (McIntyre et al., 2011). From surface explosions, variations of spectra-ratio slopes for the large amplitude laterally propagating sediment trapped seismic waves between two stations of different epicentral distances but along the same great circle path reveal seismic attenuation in one frequency band and amplification on the other. Apparently, impedance contrasts across major interfaces and lateral variations of velocity structures within the sediments including the interface between the Paleozoic basement and the overriding Cretaceous and younger sediments are responsible for the observed site-specific and frequency dependent attenuation and amplification. Thus, it is essential to explore high-resolution Vp and Vs structural models for the sediments in the upper Mississippi Embayment to understand how incoming seismic waves are amplified or attenuated from bedrock across the sediments to surface and how the effect varies between sites.

The Vs averaged to 30 m depth (Vs30) has commonly been referred to predict earthquake ground-motion amplification, and to form the basis of site hazard classification under National Earthquake Hazard Reduction Program-Uniform Building Code (NEHRP-UBC). Site-specific amplification maps have been constructed for a few basins in the US based on the soil classification and Vs30. From our recent observations, it is obvious that strong ground motion as well as site-specific seismic response in the upper Mississippi Embayment cannot be successfully evaluated simply by the general information of Vs30 and soil classifications without the involvement of reliable Vp and Vs information for the entire sediment column and their lateral variations. Furthermore, other essential elements pertinent to a successful seismic hazard assessment, such as sedimentary basin geometry, earthquake induced strong ground motion, spatial distribution of earthquake hypocenters, and characteristic feature of active faults, etc., also rely on a realistic determination of Vp and Vs structures of the sediments.

In this collaborative project, we have also learned from a comparison of seismograms recorded in the bedrock station and at a surface station that the interface between the Paleozoic bedrock and the overlying sediments is responsible for the excitation of large amplitude P-to-S (Ps) and S-to-P (Sp) converted waves. Such converted waves are dominant in the vertical (Sp) and two horizontal components (Ps) seismograms recorded on surface stations. Arrival time or travel time differences between the direct and converted waves observed on surface stations can be applied to provide important constraints for the determination of reliable Vp and Vs models for the entire sedimentary column. Using impact P-wave source, seismic reflection/ refraction profiles can be interpreted to explore Vp structure for the entire sediments. However, only Vs for shallow sediments, less than 250 m in most cases, can be determined when S-wave source is applied due to poor transmission of SH energy to the ground. As a first order approximation, Vs information for the deeper sediments can be estimated by assuming a Nafe-Drake type sediment model (Nafe and Drake, 1957; Langston 2003; Chiu et al., 2012). The final Vp and Vs models beneath each site can also be validated by comparing with nearby deep well logs, by arrival time differences between the direct and converted waves from the bottom of the sediments, and by other geological information. By integrating velocity results from this study and a few other previous studies, reliable 3-D Vp and Vs models for the post-Paleozoic sediments throughout the broader upper Mississippi Embayment can be determined. Site-specific amplification closely related to the high impedance contrast, predicted strong ground motion from potential future earthquakes, 3-D basin response, crustal structure, earthquake hypocenters, and the geometry of active faults in the embayment can thus be better evaluated.

Background

The New Madrid seismic zone (NMSZ) (Figure 1) is currently the most seismically active region in the United States east of the Rocky Mountains (Johnston, 1982). Potential for future damaging earthquakes along the NMSZ is the highest in the central and eastern U.S. The active seismic zone lies beneath the thick sediments in the upper Mississippi Embayment. Site response, sedimentary basin geometry, earthquake induced strong ground motion, distribution of earthquake hypocenters, and geometry and characteristic features of active faults are among the most essential elements for a successful seismic hazard assessment in the upper Mississippi Embayment. These elements cannot be successfully evaluated without reliable Vp and Vs information for the entire embayment sediments.

We have learned from a few recent large damaging earthquakes that local soil conditions can have a profound influence on the characteristics of ground shaking during a large earthquake, e.g. the 1985 Mexico, the 1988 Armenia, the 1989 Loma Prieta, the 1994 Northridge, the 1999 Chi-Chi, Taiwan, the 2001 Gujurat, India, the 2011 Christchurch, New Zealand, and the 2011 Tohoku, Japan earthquakes. These examples highlight the importance of how local soil conditions affect ground motions responsible for damages and casualties. As a first order approximation, site specific soil classifications and Vs30 information have been adapted by NEHRP as the standard to estimate site amplification and to predict strong ground motion, e.g. Cramer (2001, 2006), Gomberg et al. (2003), and Cramer et al. (2004) for seismic hazard maps in the Memphis and embayment area; Williams et al. (1997) for Seattle, Washington; and Wills et al. (1998) for large scale seismic hazard maps in California. In most cases, the contribution of large impedance contrasts and lateral variations of velocity structures of the sediments are not properly included due to lack of detailed and site-specific velocity information in the broader area of the embayment.

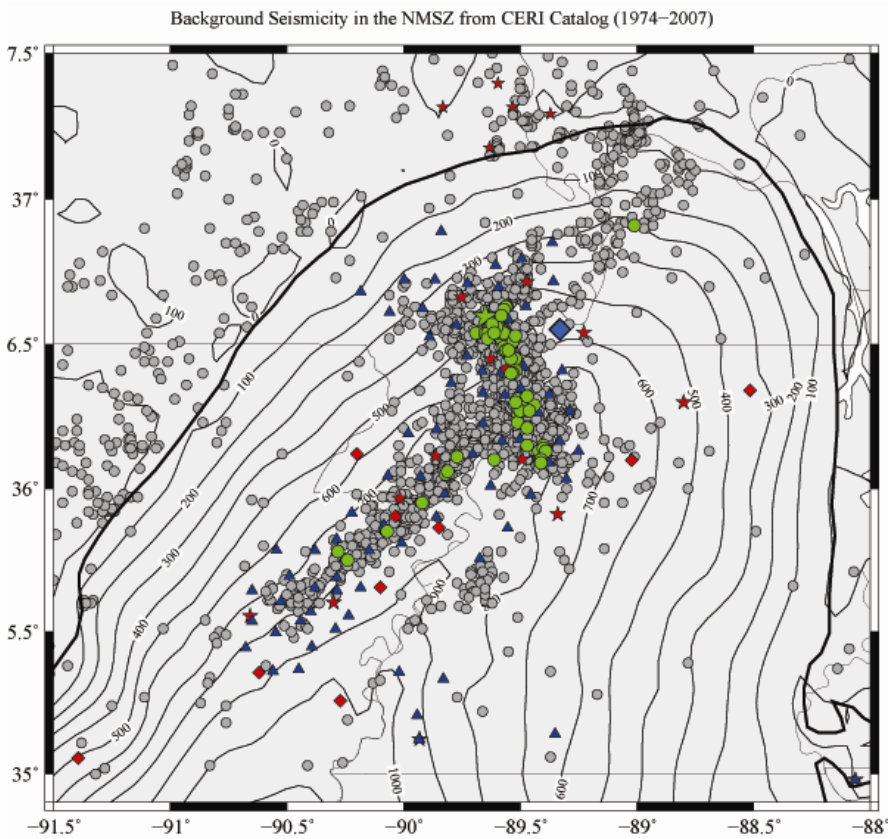

Figure 1. Background seismicity (gray circles) in the NMSZ of the central U.S along with the boundary of the Mississippi Embayment (thick line) and contour lines of the bottom of the sediments (thin lines). Solid green circles are recent earthquake locations during the period of previous broadband deployment. Red diamonds are the locations of deep wells with logs that reach to the bottom of the sediments. Blue triangles and red stars are the short-period and broadband CERI network stations, respectively. Blue diamond is the location of UK's deep drilling site near Hickman, Kentucky where the Paleozoic basement is reached at 593 m from the surface.

The sedimentary basin in the upper Mississippi Embayment is a south-plunging synclinal trough, characterized by gently south dipping post-Paleozoic sediments that thicken southward and toward the central axial line of the embayment (Figure 1). Within the sedimentary basin, significant lateral and vertical variations of sediment properties are commonly observed from a few deep well-logs (Dart, 1992; Gao 1999). Results from a few shallow seismic lines conducted in the mid to late 90s by the University of Kentucky (UK) near the New Madrid area (e.g. Street et al., 1995) further reveals that the large impedance contract across an interface at ~100 m (Figure 2) may be responsible for the significant amplification beneath these sites. The depth and impedance contrast of the interface varies slightly even though these sites are relatively close together. Sedimentary basin behaves as a perfect waveguide to retain seismic energy and to amplify vertically or laterally traveling seismic waves of certain frequencies that cannot be successfully interpreted simply from information of Vs30 and near-surface soil classification alone. Characteristic features of the sedimentary basin in the embayment, therefore, cannot be adequately represented simply by a 1-D homogeneous horizontally layered model that is used for routine earthquake location (e.g. Chiu et al., 1992; Dorman and Smalley, 1994; Chiu et al., 1997). Future

improvement for seismic hazard assessment in the upper Mississippi Embayment will have to rely on better-determined 3-D Vp and Vs models for the entire sedimentary basin.

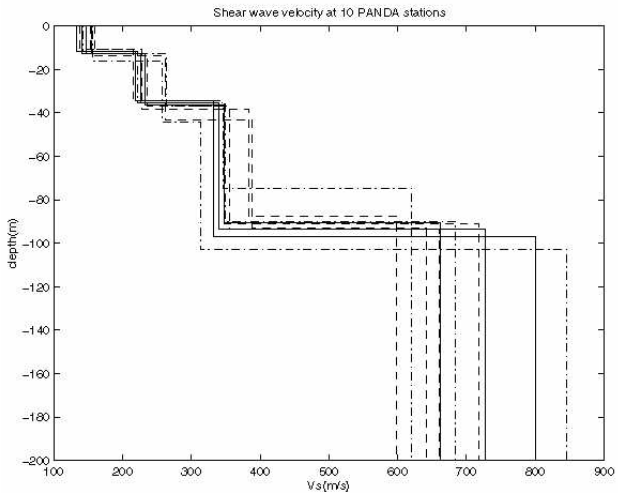

Figure 2. Shallow Vs profiles from seismic reflection/refraction lines near 10 PANDA stations showing that Vs is slower than the speed of sound in air in the upper most 100 meters of sediments. Very significant depth variations of the interfaces and interval Vs are apparent even when these sites are adjacent to each other. The large impedance contrast across the sedimentary layer boundary at a depth ~100 m will most probably contribute to the most significant site-specific amplification for the incoming seismic waves.

Many previous studies of velocity structures of the sediments in the embayment are either focused on shallow (less than 100 m), or relatively confined in small areas directly above or nearby the active seismic zone, or along a few lines across the embayment that leave a large area of the embayment un-sampled. The proposed study of Vp and Vs structure of sediments at all the 13 USAarray sites and existing regional seismic network stations will provide a unprecedented opportunity to explore structural information of previously un-sampled regions. 11 sites around broadband regional seismic network stations will provide denser sampling of regions directly above the active seismic zone. By integrating Vp and Vs information of the sediments beneath selected sites and shallow velocity information at many other sites from many previous studies, representative regional 3-D Vp and Vs models for the upper Mississippi Embayment sediments can be constructed, from which site specific amplification factors, predicted strong motions, and seismic hazard maps for the upper Mississippi Embayment can be more reliably evaluated.

In addition, earthquake-induced ground motions in the upper Mississippi Embayment are expected to be predominantly a function of attenuation (Q) in the deeper velocity structure, and a function of shear-wave velocities and vertical and lateral variations of properties of the near-surface soils (Street et al. 2001; Williams et al. 2001). However, unexpected strong ground motions from a moderate to large earthquake (Mw≥ 6) could be produced from P/Sv wave coupling of non-vertically incident waves, trapped body waves, locally generated surface waves arising from the conversion of S-waves to surface waves at the boundary of the sediment-filled basin (Frankel et al. 2001), spatial variations caused by irregular geometry in the bedrock-sediment interface, and/or horizontal variations in the seismic velocity and density, focusing effect by the geometry of the basin, etc. Possible effects might also include broadband amplification, resonance at frequencies other than those predicted by 1-D modeling, and substantially longer durations in ground motions (particularly at the longer periods), such as those observed by Carver and Hartzell (1996) in the Santa Cruz Basin from aftershocks of the 1989 Loma Prieta, California, earthquake. It is also well recognized that the geometry of a sedimentary basin and the seismic velocity distribution inside it are the two essential elements that determine how the sedimentary basin responds to the incoming seismic waves. Better determination of the velocity distribution inside a sedimentary basin will also significantly improve the quality of earthquake hypocenter estimations, especially the depth; from which active fault geometry and its characteristic features will be better understood. All these issues are important for a successful NEHRP program and the keys to address these issues rely

primarily on the determination of reliable Vp and Vs models for the entire sediments in the upper Mississippi Embayment.

Vp and Vs Models for Sediments in the Upper Mississippi Embayment

Previous Studies

As a first order approximation, most currently available Vp and Vs models for the embayment sediments (e.g. Chiu et al., 1992; Dorman and Smalley, 1994; Gao, 1999) are characterized by an over-simplified thin homogeneous sedimentary layer. This is due to very few direct velocity measurements in a large area and the fact that properties of the loosely unconsolidated soil, especially the upper most 100 meters, vary significantly as a function of depth and location. Although there are at least 45 deep wells (10 with lithologic and sonic logs) to the bottom of the sediments (e.g. Dart 1992; Gao 1999), they are sparsely distributed over a large area (Figure 1). Not only is there a lack of Vs information from these deep wells but also logs for the upper most 100 m (in some cases ~200 m) are usually not available. A few in-situ downhole measurements have provided direct Vp and Vs information for the very shallow sediments (e.g. Liu et al., 1997). Only a very few measurements, however, have been done outside of Shelby County, TN which constitutes only a small portion of the upper Mississippi Embayment. Recently, Vs information for the embayment was included in the CUSEC database (Bauer, 2004) but this data is also limited at very shallow depths. Therefore, a meaningful assessment of seismic response of the sediments for the upper Mississippi Embayment is hindered by the lack of broader, deeper, systematic, and reliable velocity measurements, especially Vs, for the entire basin.

It is well-recognized that the large impedance contrast across the bottom of the sediments will contribute to the first major amplification of the incoming seismic waves. The impedance contrast, especially for Vs, is also expected to be very high across the boundary between the compacted and loosely unconsolidated sediments at various depths and locations. This boundary is expected to be at different depths between sites due to different deposition history. Whether the site-specific amplification occurs at depth ~100 m as shown in the central NMSZ region (Figure 2), or at a different depth is an important topic that needs to be addressed in order to successfully estimate seismic response and the expected strong ground motion in the region.

In the mid 1980s, a layer of 0.65 km thickness with Vp=1.8 km/sec was suggested to represent the sediments in the upper Mississippi Embayment from the interpretation of a few long seismic refraction lines (e.g. Mooney et al., 1983; Andrews et al., 1985). The Vs of the sedimentary layer was introduced under an assumption of a Vp/Vs = 3.21 determined in similar sediments elsewhere. From a 1-D inversion of PANDA (Portable Array for Numerical Data Acquisition) data in the central NMSZ region, Yang (1992) and Chiu et al. (1992) provided the first estimation of average Vs of 0.6 km/sec for the sedimentary layer which leads to a Vp/Vs = 3.0.

From their study of converted waves generated at the bottom of the sediments, Chen et al. (1994, 1996) concluded that incident P- and S-waves from any NMSZ earthquake will propagate almost vertically to the surface, efficiently generating large amplitude converted waves across the interface between the overriding sediments and the underlying Paleozoic basement. Chen et al. (1996) were able to estimate the variations of average Vs of the sediments, finding it ranges from 0.45 to 0.67 km/sec beneath the 40 PANDA stations in the central NMSZ. They concluded that the regions of higher average Vs could be correlated to the denser and more compact sediments in the lower part of the thick sediments. From a JHD analysis of local earthquake data, Pujol et al. (1997) pointed out that Vp and Vs of the sedimentary section is not a constant. Liu et al. (1997) shows significant differences of in-situ measurements on shallow Vp and Vs profiles of the sediments at

Shelby Forest, TN; Marked Tree, AR; and Risco, MO. In their modeling of surface wave dispersion using Vp, Vs and thickness information of the sediments from adjacent well-logs, Dorman and Smalley (1994) concluded that the sediments in the embayment serve as an excellent wave-guide to excite very efficient surface waves from earthquakes inside the embayment than from outside. Based on the relationship between the basin resonance and thickness of the basin fill, Bodin and Horton (1999) estimated an average Vs of 834 m/sec and 960 m of thickness for the post-Paleozoic sediments beneath Memphis area.

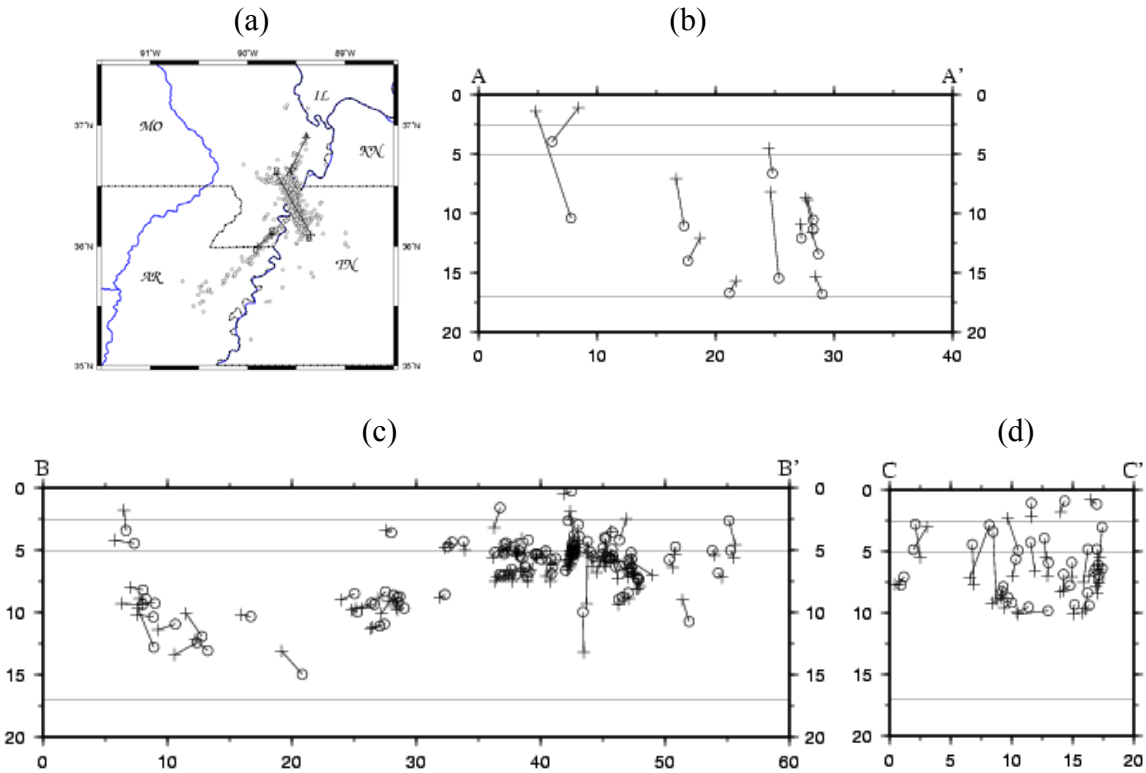

Figure 3. (a) Index map of three along-strike x-sections, hypocenters are relocated by applying a recently developed single-event location program using 3-D Vp and Vs models (Chen et al., 2006), (b) an along strike x-sectional view of hypocenters for the NE segment of the NMSZ showing the original locations (cross) and the 3D relocated hypocenters (open circle). The relocated hypocenters are, in general, shifted toward deeper depth as expected. (c) the same as (b) for the central segment of the NMSZ showing that the original and relocated hypocenters are very close to each other, and (d) the same as (b) for the SW segment of the NMSZ showing that the relocated hypocenters are consistently shifted upward.

Combining data from well-logs and from a few shallow seismic profiles, Mihills (1998) and Mihills and Van Arsdale (1999) subdivided the Post-Paleozoic sediments into layers based on lithology. Gao (1999) determined a representative 8-layer Vp and Vs model with various thickness in each layer by summarizing all the available information assuming a constant Vp/Vs ratio inside each layer based on similar lithology. In the velocity model of Gao (1999), shallow Vp and Vs information are taken from a few shallow in-situ measurements (Liu et al., 1997) and from a few nearby shallow seismic reflection/refraction lines provided by UK (Figure 2). Information about deeper S-wave velocity is determined from a linear inversion of the arrival time differences between the direct S and the S-to-P converted waves. The 3-D Vp and Vs model for the sediments has been incorporated into the initial model for a 3-D tomographic inversion to determine a 3-D

crust model beneath the upper Mississippi Embayment (Gao, 1999) and has already had a significant impact in improving the hypocentral locations (Figure 3).

Field Work

A total of 30 sites were selected in a previous and this NEHRP supported projects (Figure 4). At these sites, seismic reflection/refraction profiles using truck mounted P- and S-wave sources were conducted by the University of Kentucky group and temporary broadband seismic stations were installed by the University of Memphis group. Among them, 13 sites were located from 2006 to 2008 along two east-west lines at 36.55°N and 35.30° N latitudes and more recently, from 2010 to 2011, 17 sites in western Kentucky and northwestern Tennessee. UK's hydraulic-lift nitrogen-spring impact source can be used to generate powerful P- and S-wave sources for P- and S-wave seismic profiles at the selected sites (Figure 5). The seismic source is truck mounted for easy movement along the survey line. A 200 lb piston is accelerated by a 3000 psi gas spring to generate seismic waves to sample sedimentary interfaces to 1000 m for P and 300 m or less for S. The penetration depth of the S-wave is limited due to poor coupling of the steel base plate with the ground for lateral vibration. Locations of seismic reflection/refraction are shown in Figure 4 and are listed in the attachment A. Local, regional, and teleseismic earthquakes were recorded continuously with 100 samples/sec at all temporary broadband stations. Data recorded at these sites are also analyzed to determine arrival time differences between the direct and converted waves from the bottom of the sediments. Brief results from the analysis of seismic profiles are summarized below.

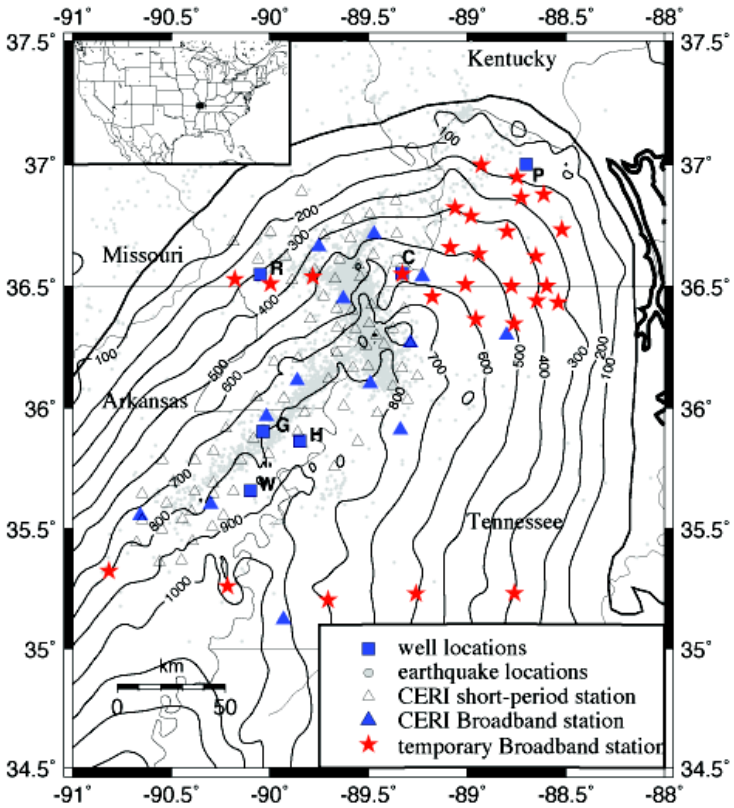

Figure 4. Map showing the locations of 30 selected sites in the previous NEHRP projects where temporary broadband seismic stations were installed (solid red stars). Short seismic reflection/refraction profiles using P- and S-wave sources were conducted at these sites. The recently installed deep borehole site (CUSSO) near Hickman, Kentucky by the University of Kentucky group is shown as a solid red square. Seismicity of the NMSZ (grey circles), short-period (open triangles) and broadband (solid blue triangles) regional seismic network stations are shown in the background.

Figure 5. Truck mounted P-wave (left) and S-wave (middle and right) sources. A 200 lb piston is accelerated by a 3000 psi gas spring to generate P- and SH-seismic waves when the impact is perpendicular and 45º, respectively, to the steel base plate coupling tightly to the ground.

Interpretation of Seismic Profiles

The P- and SH-wave field files are processed on PCs using the commercial software package VISTA 7.0 (Seismic Image Software Ltd., 1996). Typical signal processing consists of converting the raw files into SEG-Y format files, bandpass filtering, applying an automatic gain control (AGC), and using a frequency-wave number (FK) filter to remove residual ground roll. Timing corrections due to changes in elevation between the shot points and geophones will be included at sites with significant relief. The two-way intercept times and stacking velocities from interpreted P- and SH-waves reflections will be estimated using an interactive hyperbolic curve-fitting computer algorithm for the X^2-T^2 analysis. Interval velocities are then calculated using the Dix equation. First-break arrival times for the refracted SH-waves are interpreted by the seismic-refraction software package SIPT2 v.4.1 (Rimrock Geophysics, Inc., 1995) to derive the S-wave velocity-depth model. SIPT2 uses the delay-time method to obtain a first approximation of the velocity-depth model by comparing the observed first-break picks to those computed using ray tracing. The model is then iteratively adjusted to decrease the travel-time differences between the first-break picks and the model-calculated arrival times.

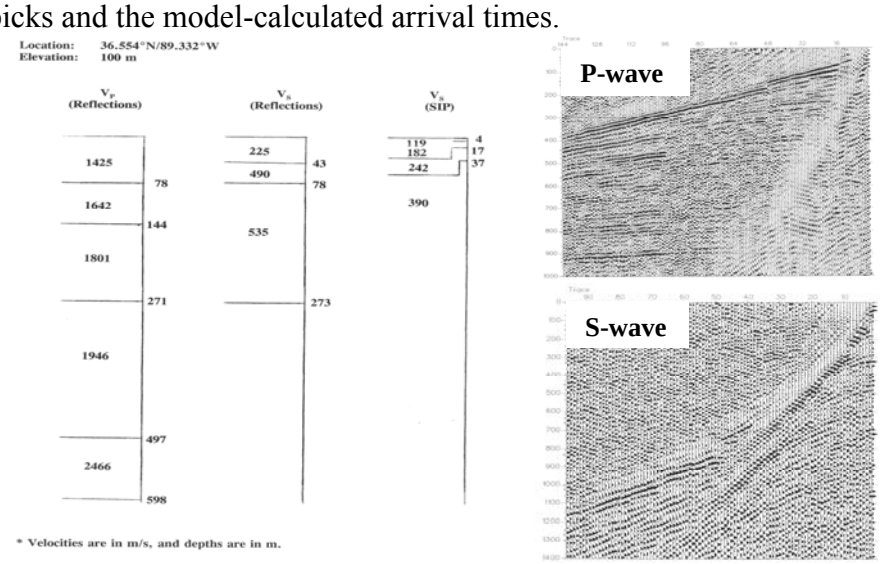

Figure 6. (Left) P- and S-wave velocity/depth models (depth shown along the side of column; no elevation correction) for the unlithified sediment near the UK's borehole array site in Hickman, Kentucky, (Right) Example of reflection/refraction seismograms used to derive the models shown to the left.

Examples of P- and S-wave seismic profiles collected at a site near the Hickman borehole array and interpreted Vp and Vs models are shown in Figure 6. In this example, the Vp model for the entire thickness of sediments has been resolved but only the top 273 m of the Vs model. Summary of the interpreted Vp models and Vs models from the existing sites (Figure 4) along 36.6° N and 37.1º N latitude lines are shown in Figure 7. It is consistent that the entire sediments are sampled at all sites using P-wave source. Paleozoic bedrock with Vp 5.9~6.0 km/sec is consistently detected at different depths at different stations. Sediments are relatively shallow along the 37.1ºN line that most Vp and Vs models are resolved. However, only shallow Vs models are resolved at most sites of thick sediments along the 36.6ºN line except a few sites near the eastern and western boundary of the embayment where sediments are relatively thin. Nevertheless, Vp and Vs models along this east-west latitude line in northern embayment show very significant lateral and vertical variations of structural model for the sediments. Such structural complication will definitely have significant affects on the observed ground motions from laterally and vertically propagating seismic waves.

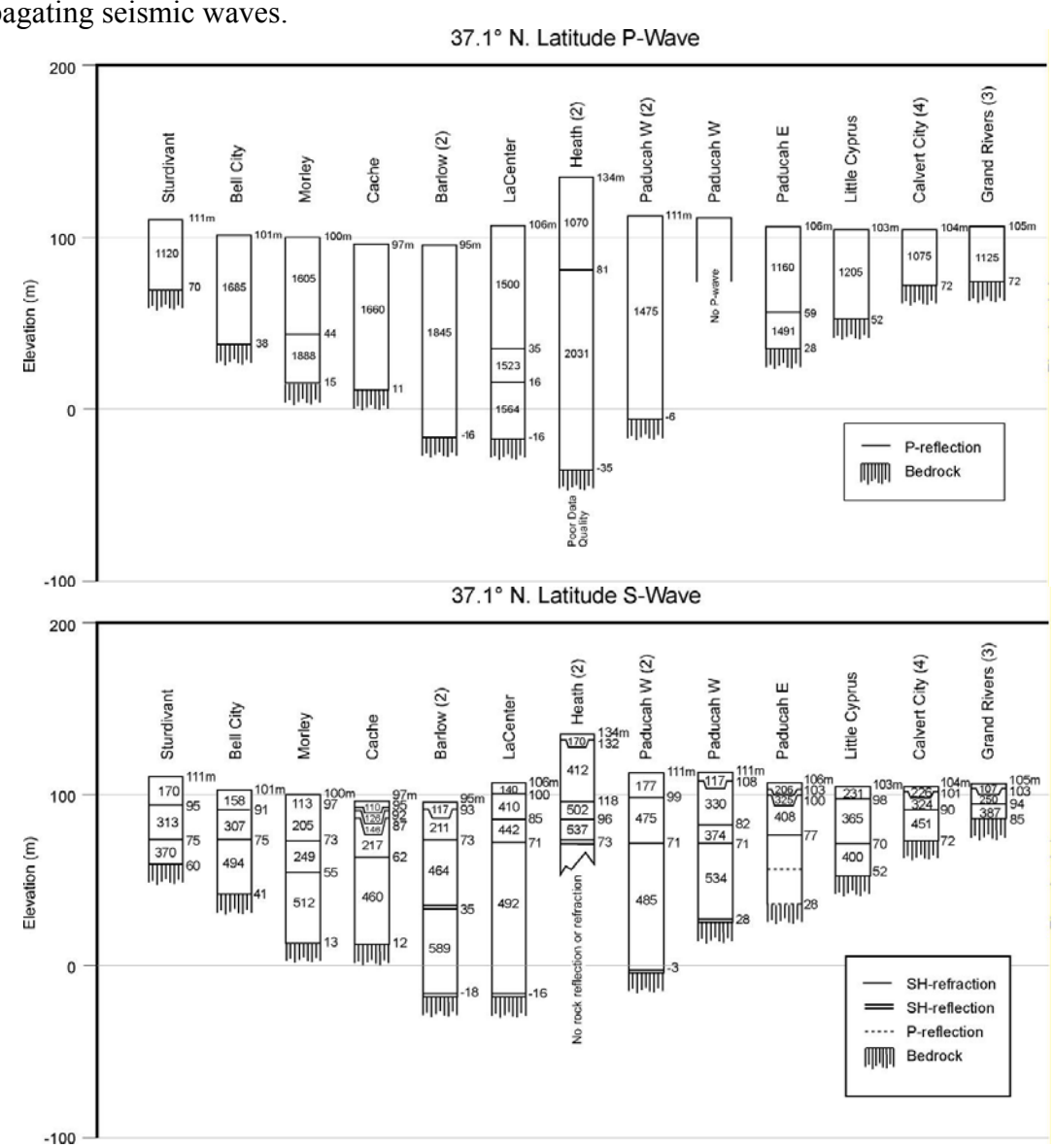

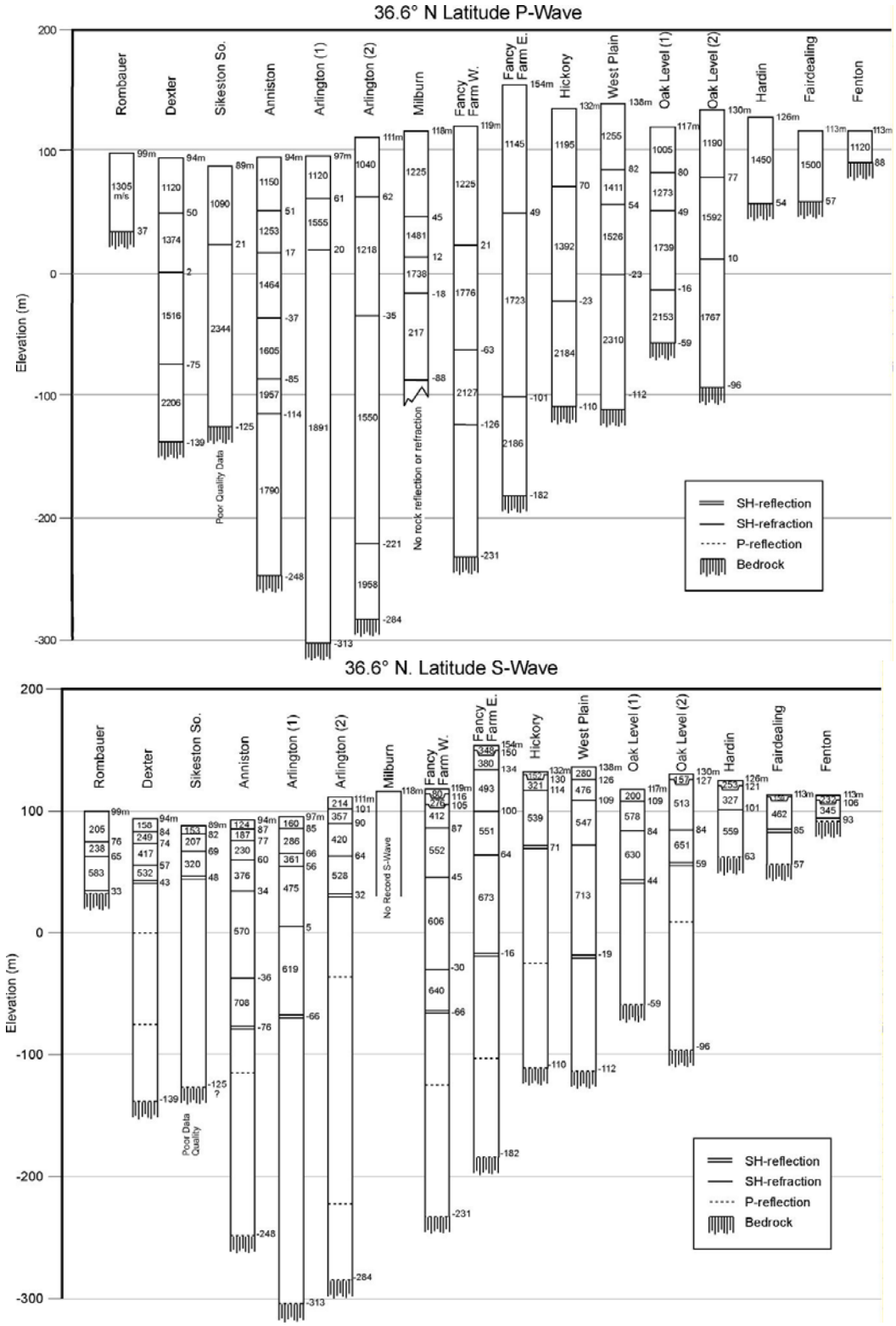

Figure 7. Summary of the interpreted Vp and Vs models for sites in southeastern Missouri and western Kentucky along the 37.1ºN (top two) and 36.6° N (bottom two) latitude line in the northern Mississippi Embayment. Structural models for the entire sediments including the Paleozoic bedrock all sites are sampled using P-wave source. Along the southern line, only shallow structures are resolved using S-wave source mainly due to weak SH wave generated from poor coupling between the plate and ground.

Penetration depths of SH waves vary at different sites depending on mostly soil and site conditions. At all sites, bottom of the sediments or top of the Paleozoic basement can also be determined from linear interpolation and extrapolation of existing deep well logs as well as from the travel time differences between the direct and converted waves observed throughout the embayment. Figure 8 shows that geometry of the bottom of the sedimentary basin is in good agreement between well logs and converted wave study as well as from the seismic profiles. The Paleozoic basement is characterized with a Vp of 5.9 ~ 6.0 km/sec that is consistent from the Vp profile, occurring at different depths beneath different sites. As shown in Figure 7, significant lateral and vertical variations of Vp and Vs, especially in the upper most 200 meters, are apparent as shown in these examples.

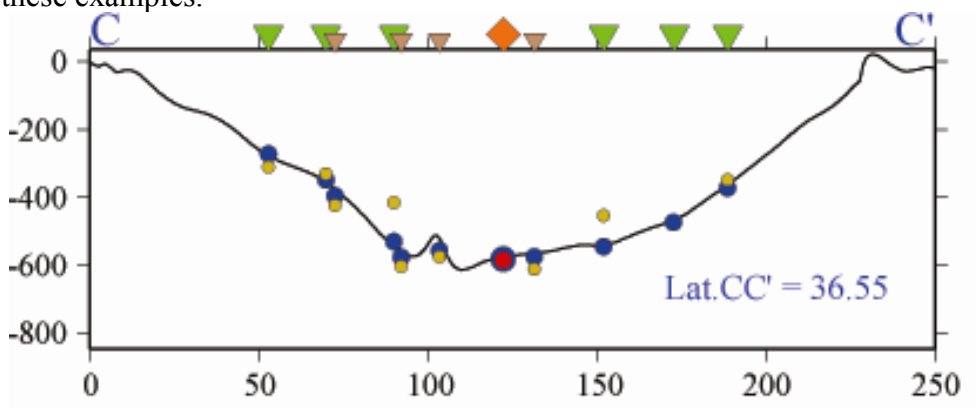

Figure 8. An EW cross-sectional view of sediment profile showing the locations of the six selected sites (reverse green triangles), the CERI seismic station sites (reverse pink triangles), and the UK's borehole site (orange diamond). Top of the Paleozoic basement from the contour lines shown in Figure 1 is marked by the blue line. Bottom of the sediments estimated from well logs and from the converted wave study is marked by solid blue and yellow circles, respectively.

Deeper Vs Models for Sites of Thick Sediments

Since the S-waves generated by the new shear-wave source are not capable of sampling sediments deeper than 300 meters due to the limitation of the coupling of the plate to the ground, we first determine Vs information for the deeper sediments following a linear inversion technique of Gao (1999). With the known thickness of sediments, Vp model, and Vs model for the upper 300 m, the Vs model for the deeper sediments can be inverted using a simple linear inversion of travel time differences Δt_{S-S_p} as *a priori* information. As shown in Figure 9, deeper Vs structure can be obtained from this linear inversion that are in good agreement with the constraints of site-specific travel time differences between the direct and converted waves. However, the inversion results, i.e. deeper VS information, are subjected to the problem of "non-unique solution". Alternatively, we intend to try another approach by assuming a Nafe-Drake type sediment model (Nafe and Drake, 1957; Langston 2003; Chiu et al., 2012) as shown in equations (1) and (2).

$$\rho = (1-\phi)\rho_S + \phi\rho_W$$

$$V_P^2 = \frac{\rho_S}{\rho}(1-\phi)^5 V_{Ps}^2 + \phi(1+\frac{\rho_W}{\rho}(1-\phi))V_{Pw} \qquad (1)$$

$$V_S^2 = (1-\phi)^n V_{Ss}^2 \qquad (2)$$

Porosity (φ) is derived from the observed P wave velocity (V_p), an assumed solid model P wave velocity (V_{Ps} 6.1 km/s), water P wave velocity (V_{Pw} 1.5 km/s), solid model density (ρ_s 2.7 g/cc), and water density (ρ_w 1 g/cc); Shear wave velocity (Vs) is derived from an assumed solid model shear

wave velocity ($V_{Ss,}$ 3.5 km/s) and resulting porosity (φ) with exponential power of 5.6 as suggested by Langston (2003). Again, travel time difference Δt_{S-S_p}, unique for each site, will be used to verify the resultant Vp and Vs models of the sediments. This process is in progress and will be reported in a paper soon.

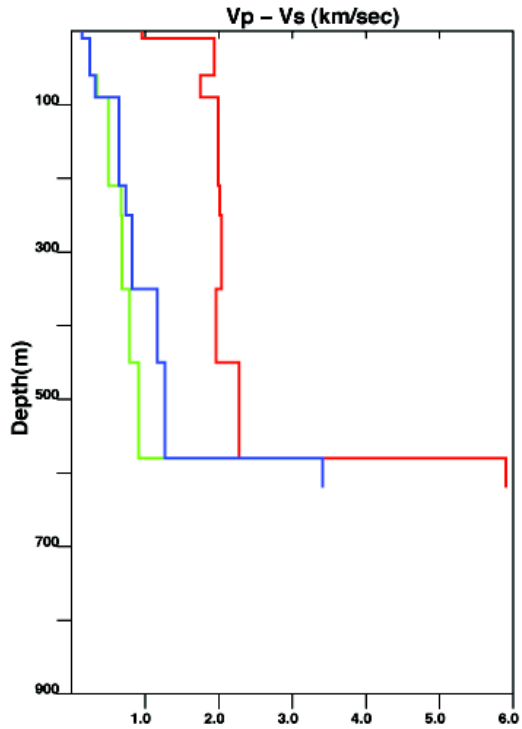

Figure 9. Examples showing a Vp profile (red line) from well logs and a seismic profile, an initial Vs model (green line) from a seismic profile and surface wave study, and the final Vs model (blue line) using the linear inversion technique of Gao (1999). The top three layers of the initial Vs model are determined from a seismic profile while the bottom five layers of the initial model are adapted from the surface study of Dorman and Smalley (1994). The final Vs model is determined based on a known Vp profile, shallow Vs, and time difference between the direct and converted waves.

Wave Conversion and Site-Specific Amplification from the CUSSO Borehole Array

Background

Short-period and broadband regional seismic network stations and many temporarily deployed seismic stations in the embayment are mostly on the surface or at very shallow depths. Therefore studies of seismic response of sediments in the Mississippi Embayment depend mostly on surface observations until recently when the Central US Seismological Observatory (CUSSO) was installed by the University of Kentucky near Hickman, Kentucky. The CUSSO borehole array consists of 5 strong motion sensors (two FBA-23, two EA-120, and one Hypo Sensor) at depths of 0 m (surface), 30 m, 260 m, 512 m, and 593 m. The station at the bottom is located within the Paleozoic basement rock. The surface and bottom stations are also co-sited with an SP-400 broadband sensor. The installation at the CUSSO array began in late 2009 with all instruments fully operational in October 2010. All instruments are operated in trigger mode for on-site recording of local, regional, and teleseismic earthquakes. Data from this borehole array provide, for the first time in the central USA, observations from the bedrock, within the sediments, and on

the surface. These data will allow direct exploration of very important first-hand information concerning how sediments response to incoming seismic waves.

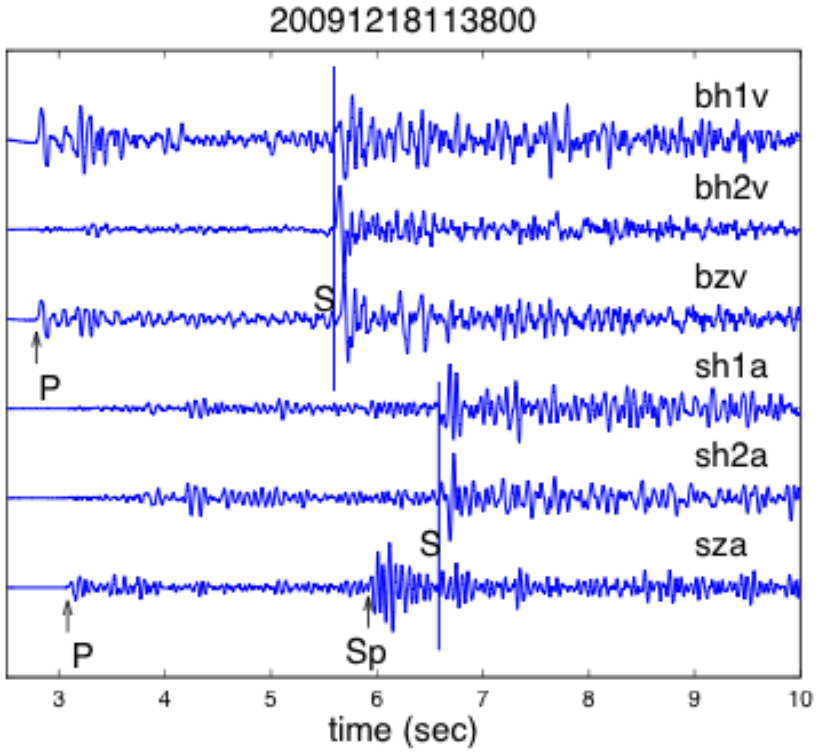

Figure 10. 3-component seismograms from a local earthquake recorded at a broadband station (upper three) at the bottom of the CUSSO array and at a surface strong motion station (lower three). Amplitude of each trace is scaled to its own maximum. The S-to-P converted wave can only be seen in the vertical component at the surface station (sza) and not in the bottom station (bzv). It confirms the interpretation of Chen et al., (1996) that the converted waves must have been generated across the boundary between the Paleozoic basement and the overriding sediments. The average Vp and Vs of the sediments can also be calculated from the P- and S-arrival time differences between the surface and bottom stations.

Wave Conversion and Average Vp and Vs of the Sediments

Figure 10 shows an example of typical three-component seismograms of a local earthquake recorded at the surface strong motion station (sza, sh1a, sh2a) and at the bottom broadband station (bzv, bh1v, bh2v). Horizontal orientations of the surface station are known but not the bottom station. Three-component seismograms recorded on the surface station are similar to those recorded at any local and regional seismic network station inside the embayment from local earthquakes. From the P and S arrival time differences between the surface and bottom stations, the average Vp and Vs of the entire thickness of sediments can be estimated to be ~2.0 km/sec and ~0.6 km/sec, respectively, that is consistent with previous reports from the converted waves (Chen et al., 1996; Gao, 1999). However, this average Vs value for the sediments is 30% to 40% lower than that determined from ambient noise studies (Bodin and Horten, 1999; Bodin et al., 2001; Langston, 2003). The differences of average Vs value for the sediments from the converted wave studies and from ambient ground noise studies was interpreted possibly due to wave conversion occurred at interfaces other than the Paleozoic–sediment boundary. However, it is apparent from Figure 10 that the S-to-P converted waves can be clearly identified on the vertical component (sza) of the surface station but not at the bottom station (bzv). No visible converted

waves from deeper interfaces, e.g. Precambrian basement, can be identified in the vertical component of the bottom station (bzv). Therefore, the observations from Figure 10 confirm the interpretation of Chen et al., (1996) that dominant wave conversion takes place at the Paleozoic-sediment boundary interface and not produced by reflectors at deeper depths, e.g. the Precambrian basement, as suggested by others. In principle, the arrival time differences between the direct and converted waves are the travel time differences between the P- and S-waves across the entire thickness of sediments. Therefore, these observations provide a strong support for our effort to utilize converted waves to provide constraints on the determination of high-resolution Vs structure for the entire sediment column beneath the selected sites.

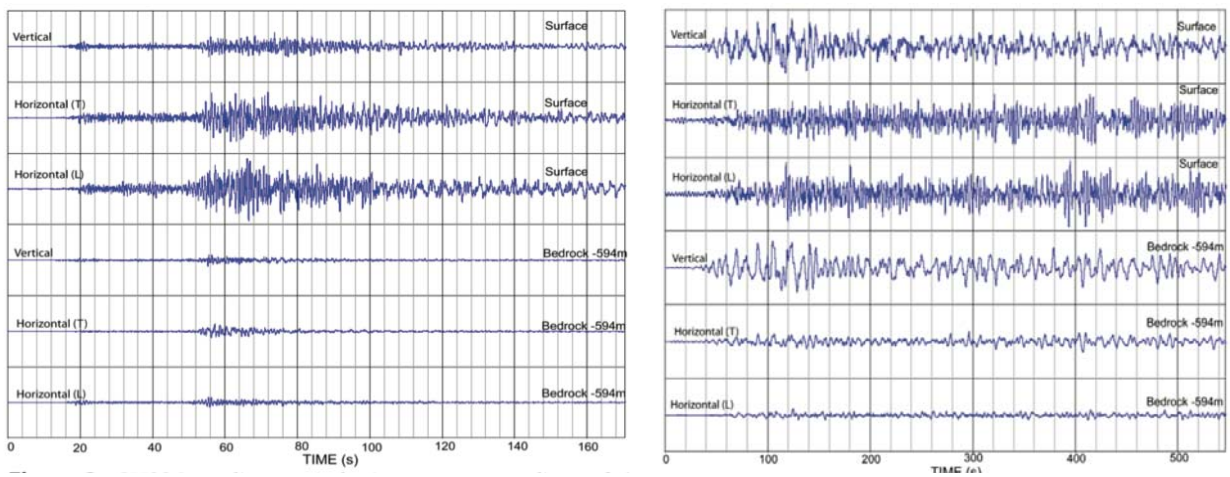

Figure 11. Vertical and two horizontal components strong motion seismograms from the 2010 M=4.7 central Arkansas earthquake (left) and the 2011 M=9.0 Tohoku, Japan earthquake (right) recorded at the surface (upper three) and bedrock station (lower three) at the borehole array near Hickman, Kentucky (Mclntyre et al., 2011). The bedrock station is located at a depth of 593 m inside the Paleozoic basement. Amplitude scale is the same within each panel. Time scale is different between the two panels. It is apparent that the amplitude of the incoming strong motion from the bottom of the sediments is significantly amplified across the interfaces of very significant impedance contrast within the sediments. It is also true that high frequency seismic waves are amplified more than lower frequency waves from large teleseismic event, revealing that amplification of seismic waves across the sediments is frequency dependent.

Frequency-Dependent Amplification of Incoming Seismic Waves

Seismic sources in the NMSZ are mostly located at depths from 5 to 17 km beneath the embayment sediments. Because of lack of direct observations at the bottom of the sediments, it is, however, not well understood as how incoming seismic waves are amplified or attenuated vertically or horizontally across the sediments. The borehole recordings at the CUSSO site in western Kentucky have provided, for the first time, an unprecedented opportunity to use direct observations to evaluate qualitatively amplification of seismic waves of various frequencies from bedrock across the entire overriding sediment. Examples of 3-component seismograms from a regional and a teleseismic earthquake recorded at the surface and bedrock stations are shown in Figure 11. The differences of seismograms between surface and bedrock stations are apparent and dramatic in both regional and teleseismic waveforms. High frequency seismic waves from the M 4.7, October 2010, central Arkansas earthquake at regional distance are amplified more than 10~15 times from the bedrock station across ~593 m of sediments to the surface station. However, low frequency seismic waves from the M 9.0, March 11, 2011, Tohoku, Japan earthquake are amplified only 2~3 times,

much less than that from the regional earthquake. Therefore, site response of the sediments beneath any site in the embayment depends on frequency contents of the incoming seismic waves. Spectra ratio between seismograms recorded at the surface or at other depths within the sediments and at the bedrock station will provide a transfer function for various parts of the sediments. Transfer function can also be calculated from the derived Vp and Vs models of the sediments. Detail analyses of transfer function of the sediments from borehole seismograms and from velocity models are in progress and will be presented in a paper later.

Average Vs of the Sediments in the Upper Mississippi Embayment from Converted Waves

Background

Very strong S-to-P (Sp) and P-to-S (Ps) converted waves from local NMSZ earthquakes are commonly observed at all three-component seismic stations within the upper Mississippi Embayment (Figure 12). The converted Sp and Ps waves are most prominent at the vertical and two horizontal components, respectively (Figure 12). The impedance contrast between the Paleozoic basement rock (Vp ≈ 5.9 km/s) and the overlying sediments (Vp ≈ 2.2 km/s) is significant so that not only will the incoming seismic waves be amplified but also the non-vertically incident direct waves and the converted waves will propagate to the surface almost vertically. Thus, the variations of arrival time differences (Δt_{S-S_p} and Δt_{P_s-P}) can be interpreted to correspond to the difference in thickness and velocity characteristics of the sediments beneath each station. We will focus on the Sp phase because its arrival time is easier to pick on the vertical component than that for the Ps phase on the two horizontal components.

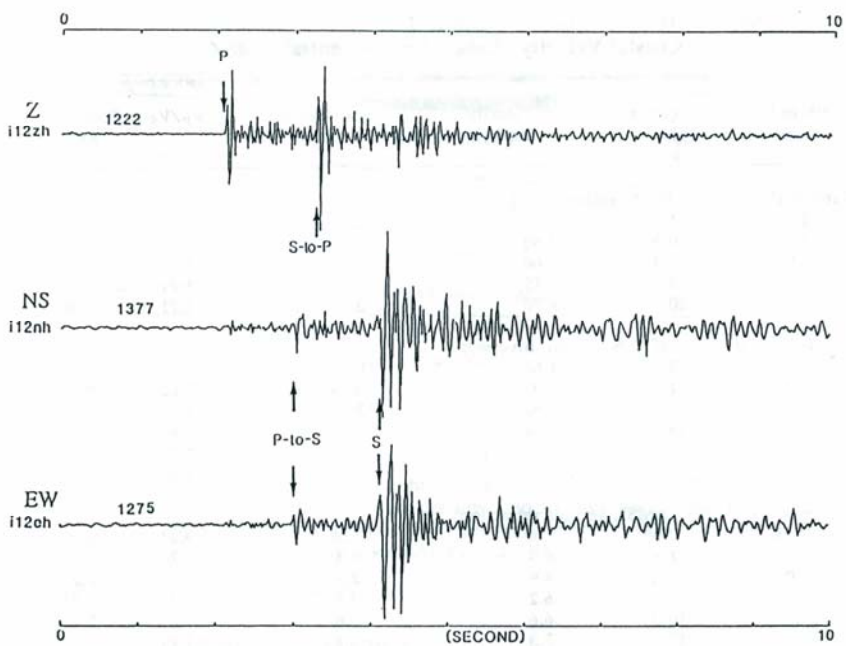

Figure 12. Typical three-component digital seismogram of a central NMSZ earthquake recorded at a PANDA station. Direct P is unambiguous on the vertical as well as is direct S on the horizontal components. The two strong signals arriving between P and S are interpreted as an S-to-P converted wav (vertical component) and s P-to-S converted wave on the two horizontals that are verified from the borehole observation as shown in Figure 10.

Chen et al. (1994; 1996) reported that the arrival time differences between the direct and converted waves from the bottom of the sediments are constant for a seismic station, but are different at different stations as shown at three CERI stations in Figure 13 where Δt_{S-S_p} for all earthquakes recorded at the same site are plotted against either epicenter distance, or azimuth, or depth of earthquakes. Therefore, a representative Δt_{S-S_p} for each selected site can be determined from a least-square fit of data similar to that shown in Figure 13. The representative Δt_{S-S_p} for each site can be used to validate the interpreted Vp and Vs models. We have estimated sediment thickness from well log data and for the determination of representative Δt_{S-S_p} values for CERI permanent and temporarily deployed seismic station sites. Results from these studies have provided important constraints for the interpretation of Vp and Vs models from seismic lines and to verify the resultant Vp and Vs profiles beneath each site.

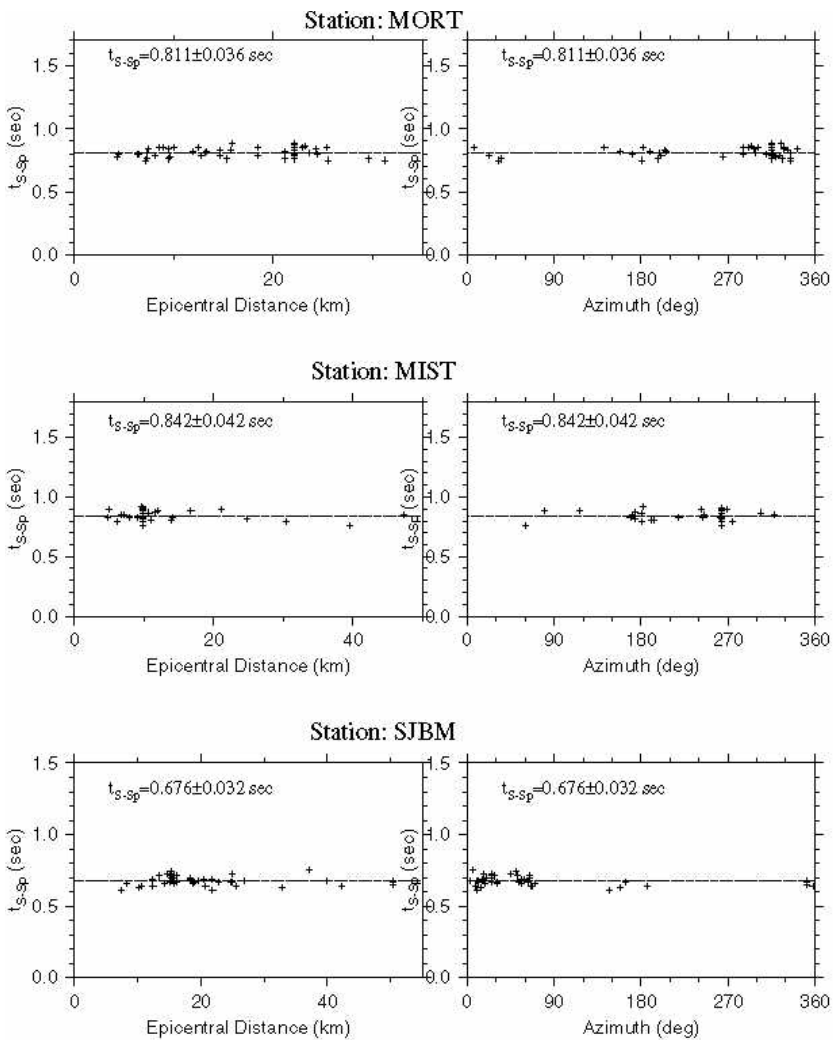

Figure 13. Plots of travel time difference (Δt_{S-S_p}) between the direct S and converted Sp waves versus epicentral distance (left) and azimuth (right) of earthquakes for three CERI stations showing that Δt_{S-S_p} is a constant for each station independent of the distances and azimuths of the earthquakes but are different between stations.

Averge Vs for the Post-Paleozoic Sediments in the Upper Mississippi Embayment

Since Vp in the sediments ranges from ~1.8 km/sec at shallow depth to 2.2 km/sec near the bottom of the sediments, an assumption of average Vp of 2.0 km/sec for the post-Paleozoic sediments is a reasonable approximation. Sonic log data are available from 10 deep wells that penetrate into Paleozoic rocks beneath the sedimentary basin (Dart 1992). In addition, 35 deep wells (without logs) can also provide important constraints on the thickness of the sediments or depth to the top of Paleozoic rocks. Thickness of the sediments beneath each selected site can be estimated from an interpolation or extrapolation of information available from these 45 deep wells using the surrounding outcrops of the Paleozoic basement as a reference (Figure 1). Thus, average Vs for the post-Paleozoic sediments can be calculated from the following equation (3).

$$\Delta t_{S-S_p} = \frac{h}{v_s} - \frac{h}{v_p} \qquad (3)$$

Where h is the thickness of sediments beneath the site; v_p and v_s are the average velocity of P and S-waves, respectively, for the sediments. Table I summarizes the observed time differences between direct and converted waves, sediment thickness, and calculated Vs beneath CERI permanent and temporary sites in the upper Mississippi Embayment. A plot of calculated average Vs versus sediment thickness is shown in Figure 14. It is apparent that regions of thicker sediments are typically corresponding to higher average Vs values that can be interpreted as a consequence of more compactness for sediments at deeper depth. The lateral structural variations of the post-Paleozoic sediments in the embayment can best be seen from the slightly scattered Vs values at sites of similar thickness. Nevertheless, a linear least square fitting of Vs and sediment thickness gives a representative empirical relationship shown in equation (4) that can be applied to estimate average Vs values for all other parts of the embayment.

$$V_s = 329.1671 + 0.4386 * h \quad (4)$$

Where h is the thickness of sediments in meters; Vs is shear wave velocity in m/sec.

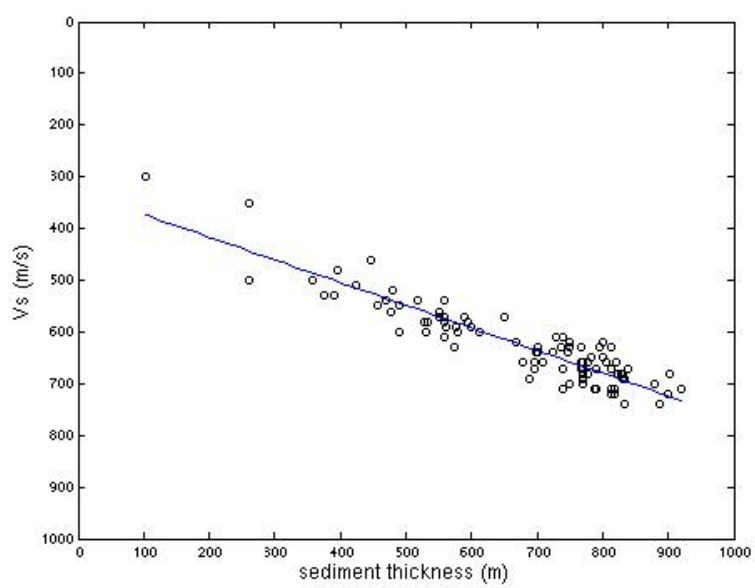

Figure 14. Plot of Vs (m/sec) versus thickness of sediments (m) using data from Table I. The least square fitting of the data gives a linear relationship between the Vs and sediments thickness. Slightly scattering of Vs values for sites of similar thickness are probably corresponding to lateral variation of local structures.

Table I

Station	Lat.(N)	Long.(W)	Ts-sp(sec)	Std(sec)	Data No.	Thk(m)	Vs(km/s)
BACM	36.724	-89.865	0.615	0.034	20	260	0.35
CATM	36.613	-89.647	0.655	0.056	32	532	0.58
COKM	36.711	-89.726	0.545	0.062	36	391	0.53
LEPT	36.299	-89.461	0.746	0.04	62	698	0.64
BETM	36.612	-90.059	0.388	0.027	24	261	0.5
RELT	36.033	-89.302	0.731	0.033	9	770	0.69
CPAR	35.556	-90.236	0.813	0.053	10	879	0.7
BLAR	35.369	-90.449	0.837	0.043	10	921	0.71
BRGM	36.205	-89.858	0.713	0.039	38	695	0.66
BROM	36.682	-90.184	0.295	0.043	17	104	0.3
CHNM	36.042	-89.929	0.759	0.054	17	777	0.68
BOAR	35.823	-90.287	0.725	0.083	13	738	0.67
CWPT	36.009	-89.626	0.715	0.051	20	833	0.74
DLAR	35.81	-90.008	0.841	0.049	11	820	0.66
DWDM	36.796	-89.493	0.52	0.032	7	375	0.53
EPRM	36.717	-89.358	0.634	0.041	22	470	0.54
FLPT	36.409	-89.321	0.722	0.043	19	708	0.66
FPST	35.978	-89.455	0.727	0.046	10	817	0.72
GLST	36.269	-89.288	0.724	0.038	55	790	0.71
GOBM	36.191	-89.979	0.746	0.08	9	667	0.62
HAWT	36.226	-89.66	0.783	0.046	39	768	0.66
HCAR	35.654	-90.38	0.777	0.024	4	725	0.64
HENM	36.716	-89.472	0.615	0.058	6	476	0.56
HICK	36.541	-89.229	0.68	0.027	5	576	0.59
HOPT	36.327	-89.376	0.721	0.027	14	813	0.72
HOVM	36.044	-90.067	0.756	0.031	10	701	0.63
KEWM	36.698	-89.593	0.599	0.038	26	456	0.55
LFRT	36.165	-89.331	0.789	0.05	39	777	0.66
LVAR	35.915	-90.222	0.692	0.057	8	697	0.67
MARM	36.53	-89.669	0.695	0.041	37	577	0.59
MATM	36.774	-89.605	0.532	0.049	8	358	0.5
MCAM	36.12	-89.702	0.786	0.041	16	791	0.67
MFRT	36.09	-89.377	0.743	0.03	7	814	0.71
MIST	36.171	-89.502	0.842	0.042	38	750	0.62
MORT	36.325	-89.566	0.811	0.036	52	749	0.63
MSAR	35.784	-90.147	0.808	0.042	12	824	0.68
MTAR	35.538	-90.442	0.797	0.006	3	829	0.68
NBNT	36.131	-89.251	0.693	0.037	6	749	0.7
NFAR	35.448	-90.393	0.878	0.039	5	902	0.68
NMDM	36.588	-89.552	0.685	0.044	19	479	0.52
NNAR	35.981	-89.823	0.826	0.039	14	838	0.67
PARM	36.664	-89.752	0.627	0.062	7	424	0.51
PENM	36.45	-89.628	0.701	0.04	13	551	0.56
PGVM	36.46	-89.729	0.706	0.027	14	517	0.54
POBM	36.409	-89.662	0.754	0.036	29	558	0.54
PPLM	36.403	-89.583	0.741	0.045	19	589	0.57
RDGT	36.246	-89.511	0.75	0.04	77	769	0.68
RSCM	36.568	-89.773	0.638	0.044	21	470	0.54

Ts-sp is the arrival time difference between the direct and converted waves; std is the standard deviation in seconds; Thk is the thickness of sediments in meters from well logs.

Table I

Station	Lat.(N)	Long.(W)	Ts-sp(sec)	Std(sec)	Data No.	Thk(m)	Vs(km/s)
SJBM	36.631	-89.476	0.676	0.032	43	578	0.6
STAM	36.331	-89.661	0.81	0.041	35	651	0.57
TIPT	36.424	-89.486	0.651	0.037	36	689	0.69
TMAR	35.695	-90.489	0.741	0.034	7	699	0.64
TNMT	36.166	-89.579	0.764	0.039	10	766	0.67
TOPM	36.526	-89.888	0.62	0.043	26	395	0.48
TWAR	35.361	-90.56	0.791	0.042	8	899	0.72
TYAR	35.509	-90.292	0.747	0.055	12	887	0.74
WADM	36.366	-89.796	0.702	0.044	33	558	0.57
WALK	36.539	-89.542	0.684	0.043	26	559	0.58
WYBT	36.348	-89.497	0.804	0.048	20	737	0.63
I01	36.383	-89.457	0.687	0.028	18	677	0.66
O01	36.5	-89.383	0.729	0.037	28	594	0.58
I02	36.705	-89.466	0.57	0	1	489	0.6
I03	36.539	-89.542	0.643	0.038	8	559	0.61
O03	36.537	-89.602	0.665	0.031	15	562	0.59
I04	36.579	-89.709	0.7	0	1	518	0.54
I05	36.536	-89.661	0.627	0.027	6	575	0.63
O05	36.615	-89.637	0.619	0.033	7	530	0.6
I07	36.449	-89.628	0.699	0.037	34	551	0.57
O07	36.476	-89.79	0.653	0.029	37	491	0.55
I08	36.494	-89.847	0.74	0.02	2	446	0.46
I09	36.364	-89.655	0.716	0.038	19	613	0.6
O09	36.429	-89.738	0.64	0.031	16	528	0.58
I10	36.341	-89.738	0.72	0.036	3	598	0.59
O10	36.202	-89.754	0.67	0.04	2	740	0.71
I11	36.311	-89.564	0.76	0.034	55	769	0.67
O11	36.361	-89.541	0.839	0.043	17	728	0.61
I12	36.321	-89.521	0.786	0.033	61	770	0.66
O12	36.268	-89.58	0.83	0	1	768	0.63
I13	36.293	-89.545	0.88	0.035	42	799	0.62
O13	36.217	-89.588	0.79	0.034	37	747	0.64
I14	36.082	-89.754	0.87	0	1	794	0.63
O14	36.007	-89.632	0.795	0.015	2	832	0.69
I15	36.112	-89.556	0.838	0.033	16	799	0.65
O15	35.939	-89.573	0.8	0.03	2	834	0.69
I16	36.299	-89.46	0.739	0.037	74	700	0.64
O16	36.188	-89.5	0.833	0.035	56	738	0.61
I17	35.979	-89.454	0.74	0.049	3	817	0.71
O17	35.987	-89.372	0.72	0.007	4	789	0.71
I18	36.136	-89.425	0.8	0.042	25	814	0.67
O18	36.083	-89.431	0.814	0.017	5	831	0.68
I19	36.11	-89.379	0.88	0.024	11	812	0.63
O19	36.033	-89.302	0.718	0.02	8	770	0.7
I20	36.22	-89.394	0.818	0.03	48	805	0.66
O20	36.265	-89.287	0.721	0.028	9	787	0.71

Ts-sp is the arrival time difference between the direct and converted waves; std is the standard deviation in seconds; Thk is the thickness of sediments in meters from well logs.

Imaging of Shallow Crustal Structure in Southwestern Kentucky by Using Microearthquake Waveforms*

(*this portion is a paper ready to submit to BSSA with authors Shu-Chioung Chi Chiu[1], Jer-Ming Chiu[1], Charles A. Langston[1], Zhenming Wang[2], and Edward Woolery[2]
[1]CERI, The University of Memphis, Memphis, TN 38152
[2]Dept. of Earth & Environmental Sciences, University of Kentucky, Lexington, KY, 40506)

Abstract

Imagings of local microearthquake displacement seismograms from P- and S-wave coda and Sp converting wave recorded on broadband stations, CUKY and HICK, are used to resolve P- and S-wave velocity structure for the unconsolidated sedimentary layer in southwestern Kentucky. Incorporated to logging data from the newly operative deep borehole CUSSO (Central United States Seismic Observatory), P-wave velocity of 2.0 km/s and S-wave velocity of 0.6 km/s can be determined to represent the average velocity structure of the entire unconsolidated sediments column in the region of southwestern Kentucky within the Mississippi embayment basin. This leads to Vp/Vs 3.3333 and Poisson ratio 0.4505 correspondently. These results are consistent to the observations of the vertical-component P and horizontal-component S waveform recorded by receivers resided at both the top and the bottom of the CUSSO vertical array. The results also agree to the Sp-to-S differential traveltime shown on the vertical- component seismogram and are similar to previous studies; however, S-wave velocity is slightly lower than that obtained in the west part of embayment and is much higher than the direct measurements from the CUSSO. It is suggested that accuracy of the logging data needs be re-evaluated. Five major reflectors which are identified within unconsolidated sediments by imaging these waves agree to the result obtained from the reflection/refraction experiment conducted under a joint USGS project between the University of Memphis and the University of Kentucky. This study demonstrates the authenticity of the pseudo-imaging profiling technique.

Introduction

The New Madrid Seismic Zone (NMSZ) is the most seismically active region in the United States east of the Rocky Mountains (Johnston and Schweig, 1996). Evidences of widely distributed liquefaction from recent paleoseismological studies (e.g. Kelson *et al*., 1996; Tuttle and Schweig, 1999; Tuttle *et al.*, 2000), and repeated and relatively concentrated local earthquake seismicity reveal that potential of future damaging earthquakes in the NMSZ can not be overlooked. The Mississippi embayment, overlying much of the NMSZ, is filled with thick upper Cretaceous and younger sediments (VanArsdale and TenBrink, 2000) about 1-km thickness at the latitude of Memphis, Tennessee (Stearns, 1957; Figure 15). Site conditions of the sediments in the embayment are classified as D or higher (FEMA-450-1, 2003) in the National Earthquake Hazards Reduction Program (NEHRP). Not only the characteristics of large impedance contrast between the unconsolidated sediments and the underlying Paleozoic bedrock but also the extremely low shear wave velocity in its near-surface soils (Romero and Rix, 2000; Street *et. al.,* 2002; Rix *et. al.* 2002; Lamgston, 2003; Chiu and Langston 2009 & 2011) constitute an environment that has a significant effect on earthquake ground motion by amplifying and prolonging the shaking duration due to a major earthquake.

Ground motion amplified by the loose Ohio River deposits caused approximate $3 million damages in Maysville, KY, from the magnitude 5.2 Sharpsburg, KY, earthquake in 1980. In the central United States, many communities such as Memphis, Tennessee, St. Louis, Missouri, and

Paducah, Kentucky, are built on top of soft soils along the Mississippi and Ohio Rivers. The manifest examples (Figure 11) of recent magnitude 4.7 Guy swarm, central Arkansas, on February 28, 2011 and magnitude 9.0 Japan earthquake on March 11, 2011 show that ground motions in the upper Mississippi embayment have been amplified at least five times and, most importantly, the amplification seems to vary as a function of frequency as wave propagating from the top interface of Paleozoic rocks to the top of the unconsolidated sediments (Mclntyre *et. al,* 2011). It is evident that the corresponding strong ground motions and the site response of the thick sediments in the upper Mississippi embayment become the primary interest concerning earthquake hazard assessment in the central and eastern United States. Local site conditions in other areas have shown to influence the characteristics of the ground motions induced by great earthquakes such as the 1988 Armenia, 1989 Loma Prieta, 1994 Northridge, 1995, Mexico, 1999 Chi-Chi, Taiwan, and 2001 Gujurat, India, earthquakes. These examples highlight the urgent need of understanding the site response of soft soils in the NMSZ and its vicinity as well as their potential impact on future earthquake damages and casualties.

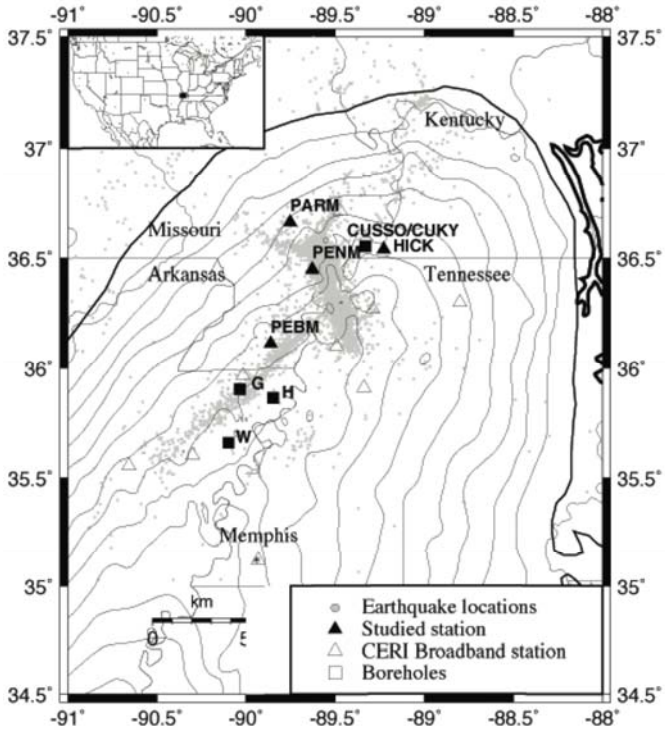

Figure 15. Location map. Contour lines represent the thickness of unconsolidated sediments in an interval of 100 meters with respect to the sea level for the upper Mississippi embayment. Both solid and open triangles are broadband stations of the Cooperative New Madrid Seismic Network operated by the University of Memphis. Solid triangles indicate stations mentioned in this and previous studies. Solid square is the deep borehole well – CUSSO operated by the University of Kentucky, and other wells – Garigan (G), Haynes (H), Dow Chemical/Wilson #1 (W) in this region. The Wilson 2-14 well is located about 100 m from the Dow Chemical/Wilson #1 well. A temporary station – CUKY was deployed at the top of the CUSSO well during February 27 – June 25, 2010. Black circles represent the locations of earthquake which waveforms are used in the analyses. Upper left corner shows an index map and black rectangle represents our study area.

Site classifications and Vs30 information (Williams *et al.,* 2003) have been adopted by the NEHRP standard (FEMA-450-1, 2003) to estimate site amplification and to predict strong ground

motions for seismic hazard maps as done in the Memphis area (Cramer, 2006), and Seattle, Washington (Williams *et al.,* 1997); however, recent geotechnical field experiments such as Vertical Seismic Profiling and Seismic Cone Penetration Tests showed that Vs profiles have little variation in the upper 30+ m (Liu *et al.,* 1997; Rix *et. al.,* 2002) while Vp increases rapidly down to the water table ~10m and retains an average of 1.8 to 2.0 km/s below (Liu *et al.,* 1997). An apparent strong-reflector at ~100 m, identified by the shallow seismic reflection/refraction experiments conducted by the UKY/UoM (e.g. Street *et al*., 2004), agrees to the results of imaging profiles using local earthquake waveforms (Chiu and Langston, 2009). It is observed that extremely low-velocity near-surface soil structure is responsible for the high frequency P and S reverberations, which can be modeled by using waveform inversion (Langston, 2003; Chiu and Langston, 2011). Therefore, geotechnical data or a simple Vs30 model may not properly predict site responses nor yield the proper wave propagation effects due to the oversimplified averaging needed for the extremely complicated shallow structure.

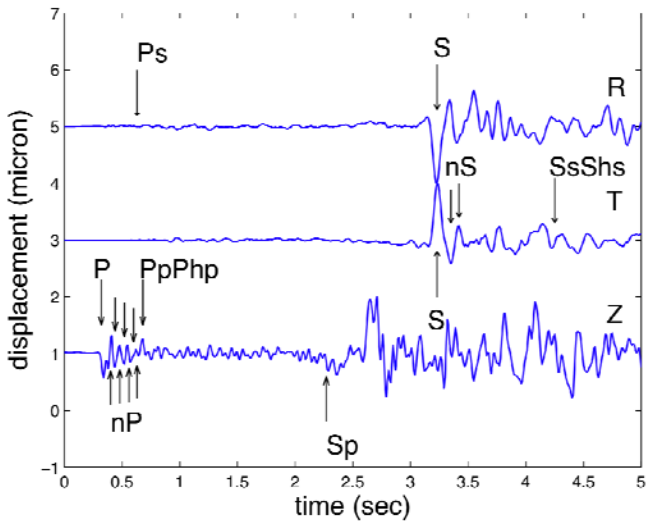

Figure 16. Typical example of displacement seismograms for a Md 2.0 Bassie. TN. earthquake occurred on April 27, 2010 @08:42:33.49. Ground motions are sampled at 100 samples/s for microearthquake recordings. The horizontal seismograms are rotated to radial (R) and transverse (T) components to facilitate the separation of P and SV motions from SH. Due to very low velocities and high Q in the unconsolidated sediments such that high frequency first reverberations of P and S (PpPhp and SsShs) waves can be observed and identified from the displacement seismograms. Major seismic phases are annotated. They are used to determine average velocities of P and S waves within sediments beneath the station. nP and nS are the resonate P- and S-wave in the near-surface soils.

About 9000 earthquakes (Figure 15) have been recorded instrumentally and arahived at the CERI earthquake catalog for the central United States since late 1974. Figure 16 shows typical displacement seismograms of a local microearthquake, which display four major features: the primary P- and S-wave, the reflected PpPhp and SsShs, the transmitted Sp from the top of Paleozoic rocks, and the reverberating nP and nS in the near-surface soft soils. Borehole array data in the new facility – the Central U.S. Seismic Observatory (CUSSO) – become available recently and form a unique set of seismic transfer functions at varying depths, which constitute an essential constraint for further waveform analyses on velocity structure interpretations. In this paper, we report the authenticity of the pseudo-imaging profiling technique (Chiu and Langston, 2009) by using local microearthquake waveform data recorded on the CUKY station along with the acoustic

logging data extracted from the CUSSO well site. The resulting velocity structure is verified by the waveform observations recorded by the vertical CUSSO array.

Velocity Structure in the Mississippi Embayment

The northern Mississippi embayment filled with thick unconsolidated sediments consists of mostly clastic sediments associated with the Mississippi River and glacial loess deposits and ranges in age from upper Cretaceous to present. The geological character of the embayment is not significantly different from other areas along the coastal plains of the southeastern United States that are covered mostly by the coastal unconsolidated sediments. Average velocity models for the large-scaled geological structure associated with Reelfoot Rift Zone have been studied by many investigators: e.g. seismic refraction/reflection techniques (e.g. Mooney *et. al*., 1983; Ginzberg *et. al.,* 1983; Catchings, 1999; Nelson and Zhang, 1991), 3-D tomographic studies of microearthquake travel times (e.g. Gao, 1999; Vlahovic *et. al.,* 2000), surface wave dispersion study (e.g. Dorman and Smalley, 1994), Vertical Seismic Profiling (VSP) (e.g. Liu *et. al.,* 1997), and the pseudo-imaging technique of local microearthquake waveform data (Chiu and Langston, 2009). Results from these studies have shown an average P wave velocity of 1.8 - 2.0 km/s in the embayment unconsolidated sediments. Furthermore, velocities gradient with sediment thickness in the embayment were also studied for P wave (Chiu and Langston, 2009) and for S wave (e.g. Chen *et. al.,* 1996; Bodin *et. al.,* 2001; Chiu and Langston, 2009; Chiu and Langston, 2011; Chiu *et. al.,* 2011). Acoustic well logs in this region are distributed sparsely. They show considerable heterogeneity with depth but havr an average P-wave velocity of 1.8 - 2.0 km/s. Note that only very few direct measurements for S-wave have been done. Recently, a deep borehole array has been installed by the University of Kentucky at the CUSSO, located at 36.5540°N, 89.3320°W down to the basement of the unconsolidated sediments with depth of 593 m. The availability of the logging information for P- and S-wave velocities (Figure 17a) within this borehole has provided essential constraints for waveform imaging in this study.

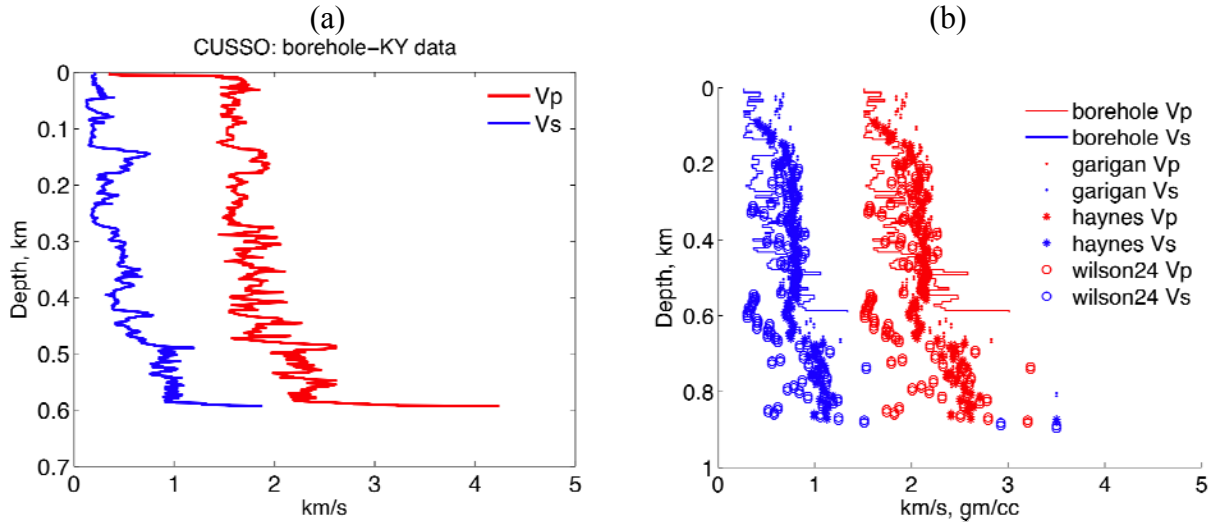

Figure 17. Well log information: (a) CUSSO Vp and Vs profiles from direct measurements of slowness starting at 2.5908 m from surface down to the depth of 592.5922 m with an average interval of 0.5 m and total sampling points of 637; (b) Comparisons of layered sediment Vp and Vs profiles among CUSSO, Garigan, Haynes, and Wilson 2-14. Vs is derived by using the Nafe-Drake type sediment model except CUSSO well. It shows that wells at four different locations display variations but in a general trend; it is noticed that Vs direct measurements profile from CUSSO deep borehole appear about half slower than others.

Figure 17b shows a collection of velocity models derived from four acoustic well logs consisting of CUSSO, Garigan, Haynes, and Wilson 2-14 where each log is represented by 100 layers. P wave slowness in each layer is determined by averaging slowness in the acoustic log over a depth range by preserving vertical travel time. Except the direct measurements of Vs at the CUSSO site, Vs for the other three sites is constructed by assuming a Nafe-Drake type sediment model as shown in equations (1) and (2).

$$\rho = (1-\phi)\rho_S + \phi\rho_W$$
$$V_P^2 = \frac{\rho_S}{\rho}(1-\phi)^5 V_{Ps}^2 + \phi(1+\frac{\rho_W}{\rho}(1-\phi))V_{Pw} \qquad (1)$$

$$V_S^2 = (1-\phi)^n V_{Ss}^2 \qquad (2)$$

Porosity (φ) is derived from the observed P wave velocity (V_p), an assumed solid model P wave velocity (V_{Ps} 6.1 km/s), water P wave velocity (V_{Pw} 1.5 km/s), solid model density (ρ_s 2.7 g/cc), and water density (ρ_w 1 g/cc); Shear wave velocity (Vs) is derived from an assumed solid model shear wave velocity ($V_{Ss,}$ 3.5 km/s) and resulting porosity (φ) with exponential power of 5.6 as suggested by Langston (2003). It appears that well logs at four different locations display lateral variations but in a general trend. Notably, Vs profile from direct measurements in the CUSSO deep borehole logging appears about half slower than others (Figure 17b). Figure 17c shows comparisons between direct measurements and derived shear velocities, as well as P wave velocity versus derived density profiles. The resulted porosity and Vp/Vs ratio are also shown in Figure 17d.

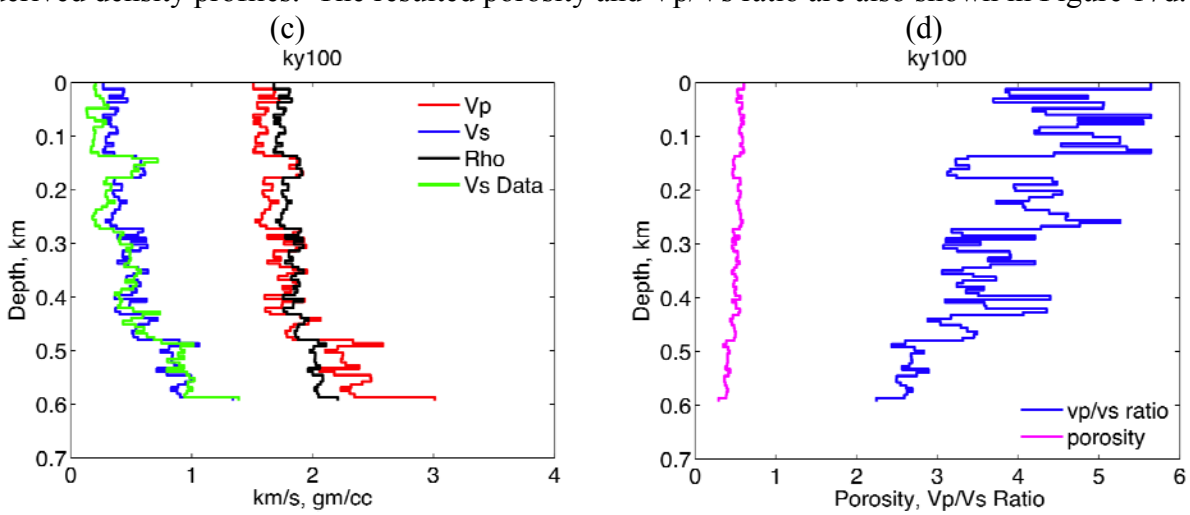

Figure 17. Well log information: (c) Comparison of observed Vp and Vs_Data as well as derived density and shear wave velocity (Vs) for the deep borehole CUSSO. Vs_Data is the reciprocal of averaging log slowness; (d) Resulting Vp/Vs ratio and porosity in CUSSO well.

Microearthquake Waveforms

A Md 3.1 earthquake occurred on 12/18/2009 @11:38:08.66 UTC located at east of Point Pleasant, MO. (36.451˚N, 89.541˚W) was recorded on the CUSSO array. Its waveform data for stations at both the top and the bottom of the array are shown in Figure 10 where major seismic phases are annotated. It is interesting to note that prominent S-to-P converted waves are visible on the surface vertical-component seismogram (sza), but are not seen on the vertical-component seismogram recorded at the base of the unconsolidated sediments (bzv). A possible surface reflected shear wave is also observed on sh2a. Based on the elevation difference as well as the

differential travel times between these two receivers, average velocities for the entire column of unconsolidated sediments in the borehole array are obtained as 1.9797 km/s and 0.5899 km/s for P wave and S wave, respectively. These results agree to the observed time separation between the direct S and converted Sp waves on the sza component. Shear wave velocity is also similar to the derived value as shown in Figure 17c. These results imply Vp/Vs ratio of 3.3560 and Poisson ratio of 0.4511.

Pseudo-imaging Profiling

The hypothesis is that microearthquake waveform data can provide an accurate view of wave propagating across the sediments. This study aims to explore the response of deep and shallow sediments due to natural earthquake ground motions and to determine a velocity representation for stations within the sedimentary basin for southwestern Kentucky. Borehole well log data and geotechnical data will provide additional constraints. Detailed procedures for data processing can be found in Chiu and Langston (2009). The summarized methodology for the pre-processed waveform data are as follows.

This method capitalizes on the fact that the unconsolidated sediments have very low velocities and relatively high Q with respect to the underlying Paleozoic sedimentary rocks so that the first reverberations of P and S (PpPhp and SsShs*)* waves can be observed and identified from the displacement seismograms. Observed primary reflections of the P and S waves and transmitted Sp wave will place strong constraints on wave travelling within the unconsolidated sediments. There are four steps involved in the imaging process: (1) the construction of an appropriate crustal velocity model; (2) the calculations of two-way and one-way travel times by using average interval velocities and ray parameter for P(S) coda and Sp wave; (3) a "Stretching" operator to convert seismic time series to a function of depth to implement the normal moveout correction and to construct a depth migrated seismic section; and (4) the identification, interpretation, and correlation of reflectors to known interfaces from nearby well logs. Normal moveout correction (NMO) is performed by (1) calculating travel times of transmitted Sp and reflected P and S waves as a function of interface depth using actual ray parameter; (2) re-sampling of time series to an equal depth interval of 0.01 km; and (3) converting time series to a function of depth by applying normal moveout correction for reflection and transmission. Pre-stacking selected waveforms may be necessary to sufficiently use this method widely.

Application: CUKY and HICK in southwestern Kentucky

We perform a 1-D migration on the local microearthquake waveform data in an attempt to image prominent reflectors in the upper crust beneath two broadband seismic stations, CUKY and HICK, in southwestern Kentucky. CUKY is a temporary station deployed at the top of the newly operative deep borehole CUSSO by the University of Memphis. HICK is a CNMSN (Cooperative New Madrid Seismic Network) permanent station. Both stations are equipped with broadband velocity sensors and located within the upper Mississippi embayment. Station and earthquake source parameters are listed in Tables 1 and 2. We select a time window from the displacement time series of P (back to Sp) and SH codas including their reverberations, and the Sp wave. In the offset-time plot, we re-sampled the displacement waveforms to an equal depth interval 0.01 km to implement the normal moveout correction. NMO migrated sections then can be as a function of depth to explore high impedance reflectors. Constrained by the direct and reflected P and S phases, transmitted Sp phase, and the thickness of sediments, common reflectors within the unconsolidated sediments and deeper geological structures can be identified. Velocity models of the CUSSO well and the Dow Chemical/Wilson #1 are adopted for P wave models of the unconsolidated sediments and the underlying Paleozoic sedimentary rocks, respectively, for these two stations. Although the P-wave velocity model is known, we will allow small adjustment to Vs in the NMO migration process so that reflection and

transmission effects can be attributed to common major interfaces among P-, SH-, and Sp- waves. Later, reflectors will be identified and correlated to known interfaces from nearby well logs.

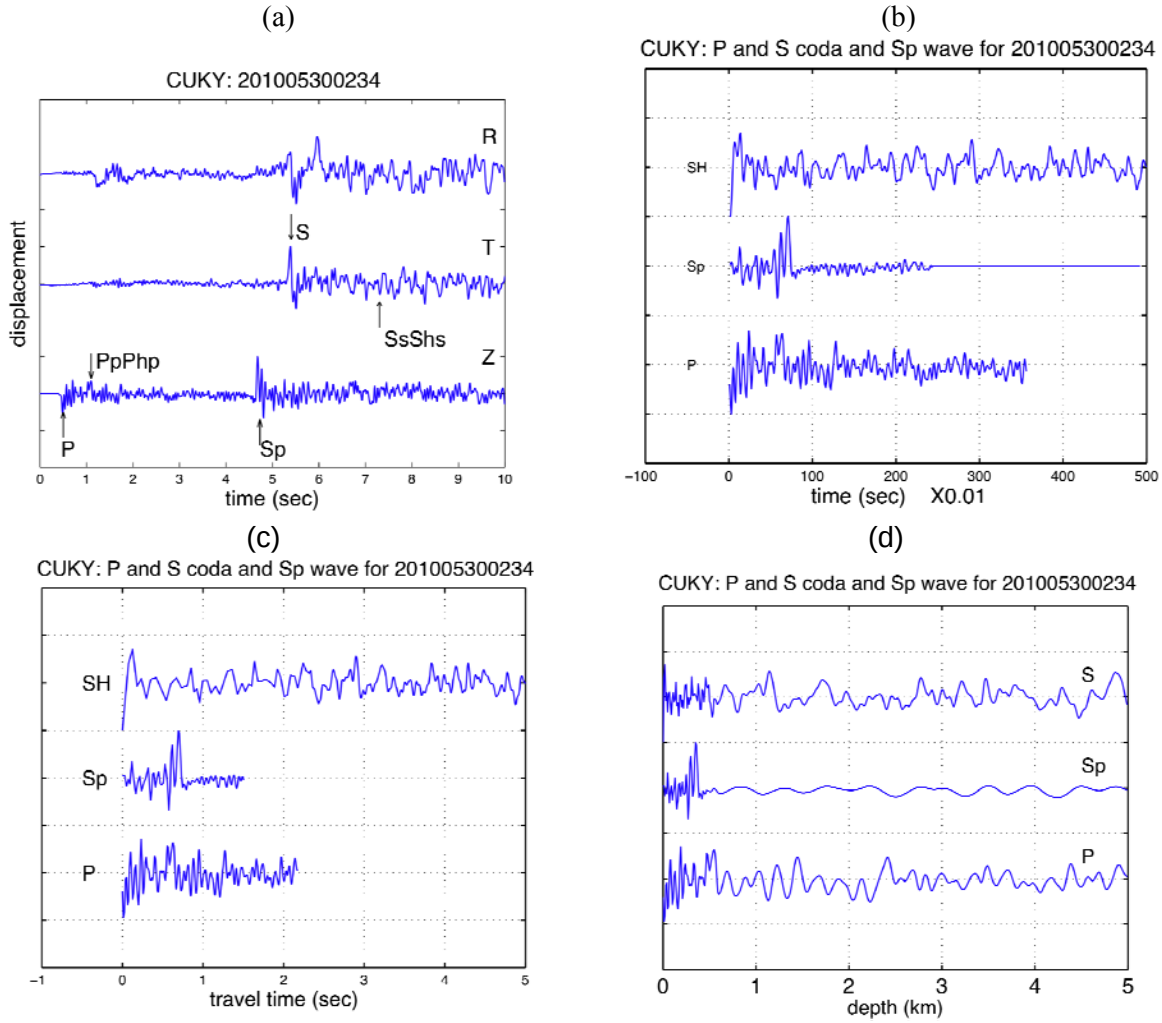

Figure 18. (a) Displacement seismograms recorded at CUKY for Md 3.1 earthquake. The seismograms are rotated to radial (R) and transverse (T) components to facilitate the separation of P and SV motions from SH. Major seismic phases are annotated; (b) P (back to Sp phase) and SH coda waves, as well as Sp converted wave displacement; (c) NMO corrected P- and SH-coda and Sp waveforms with peak arrivals at zero reference time in a function of two-way travel time for P- and SH-wave and one-way differential travel time between P- and SH-wave in sediments for Sp wave, extending to a depth of 5 km; (d) Migrated P, SH, and Sp waveforms in a function of depth. P wave is shown at the bottom trace, Sp wave is at the middle trace, and SH is at the top trace. All waveforms are normalized to their individual maximum amplitude within actual time or depth window.

CUKY

Displacement seismograms of the Md 3.1 earthquake are used in the pseudo-imaging analysis for the shallow crustal structure beneath CUKY (Figure 18a). This earthquake occurred on 05/30/2010 @02:34:01 UTC and was located at 36.5485˚N, 89.7160˚W with focal depth 9.20 km, about 1.99 km east of Baderville, MO. Its seismic imagings are processed in Figure 18b for P and S wave coda and transmitted Sp wave; Figure 18c for the NMO corrected waveform data in a function of travel times; Figure 18d for the NMO migrated waveform data in a function of depth;

Figure 18e for the migrated seismic imaging section calculated by using direct P wave velocity and derived shear wave velocity down to the depth of 5 km; Figure 18f for the migrated seismic imaging section calculated by using vp 2.0 km/s and Vs 0.6 km/s for the unconsolidated sediments and Vp 6.1 km/s and Vs 3.4 km/s for Paleozoic sedimentary rocks; Figure 18g for re-plotting top 595 m imaging section extracted from Figure 18f to depict the shallower reflectors in the unconsolidated sediments.

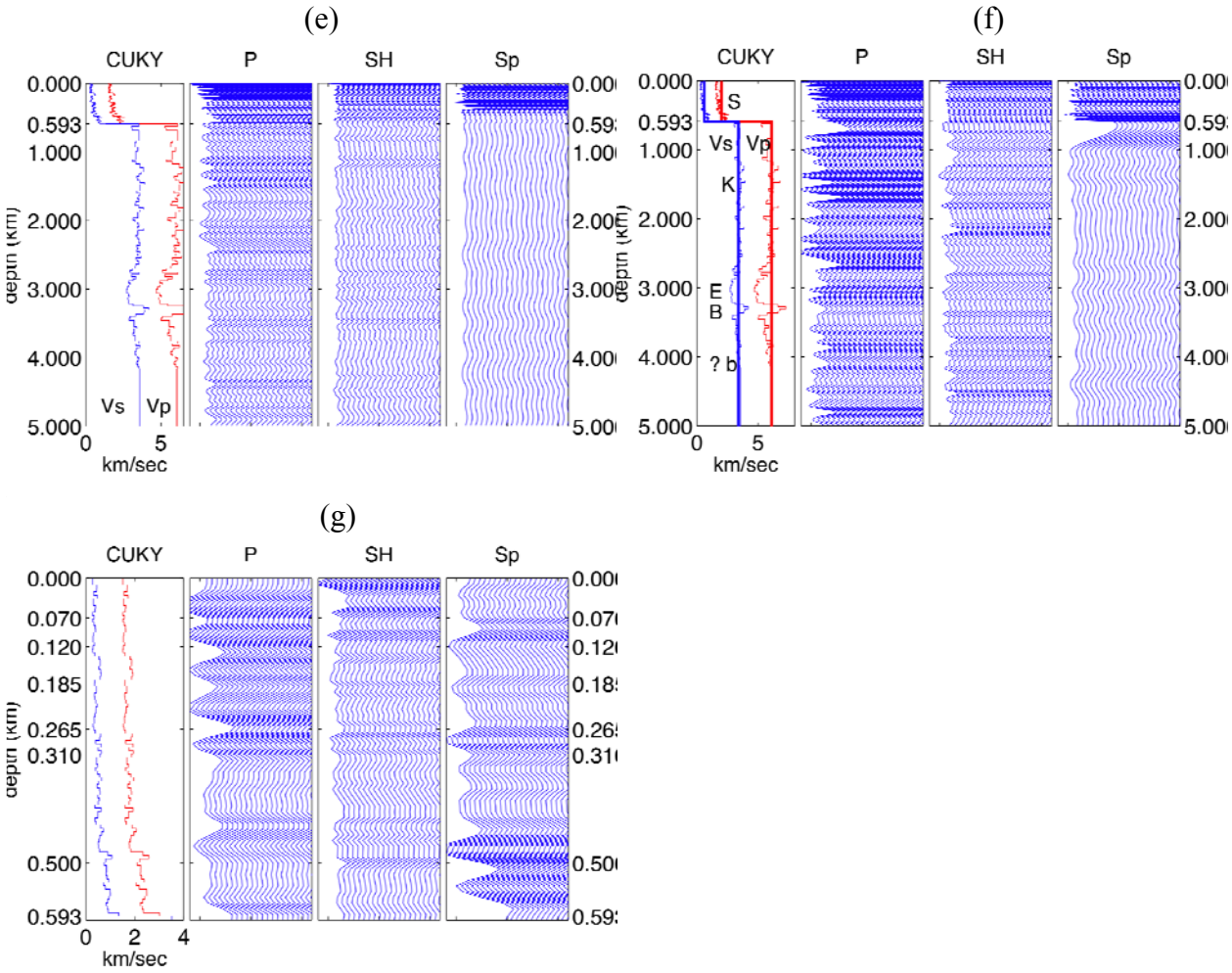

Figure 18. (e) Imaging profiles for P, SH, and Sp waves. Velocity model is included in the left panel. It consists of computed Vp using CUSSO well log data and derived Vs_data for unconsolidated sediments and Vp and derived Vs from the Dow Chemical/Wilson #1 well log data for the Paleozoic sedimentary rock. Nafe_Drake type sediment model is assumed for the unconsolidated sediments. Imaging profiles show a general pattern of reflectors among waves. However, reflectors do not line up at depth of 593 m where high impedance contrast exists between unconsolidated sediments and Paleozoic rocks; (f) NMO migrated seismic section (same format as shown in (e) constructed by using Vp 2.0 km/s Vs 0.6 km/s for unconsolidated sediments overlying a half space Vp 6.1 km/s Vs 3.4 km/s for Paleozoic rocks (thick lines). A strong reflector appears consistently well correlated to the interface at depth of 593 m among all wave types. It also displays common reflectors between P and S profiles in the deeper high-velocity image sections and associates with the stratigraphy at the nearby exploration well log. This results in vp/vs 1.7981 and Poisson ratio 0.2747 in the high-velocity Paleozoic rocks, which implies not the Poisson rocks. S: Mississippi embayment Super group; K: Knox group; E: Elvins shale; B: Bonneterre formation; b: basement; (g) NMO migrated seismic section for shallow structure extended to 0.6 km. Common reflectors can be seen at depths of 70, 120, 185, 265, 315, 500, and 593 m among waves, which agree to the results of the shallow reflection/refraction survey (Figure 19) conducted jointly by the University of Memphis and University of Kentucky (UoM/UKY) near the deep borehole site. Grey line stands for P wave and dark line stands for S wave in the velocity panel.

Despite polarity differences among P-, SH-, and Sp-waveform, this technique demonstrates that consistent reflectors in the deep sedimentary section (Figure 18f) and in the shallow unconsolidated sediments (Figure 18g) can be simultaneously imaged among the three wave types. There are excellent correlations between waveforms and reflectors associated with the base of the upper Cretaceous/Holocene Mississippi embayment Supergroup (S) as well as the base of Knox group (K) in the deeper high-velocity sections; however, it does not appear to have a clear association with the low velocity Elvins shale (E) and Bonneterre formation (B). The result shows that sedimentary structure beneath CUKY station can be represented by a layer of unconsolidated sediments of 593 m thickness with Vp 2.0 km/s and Vs 0.6 km/s atop the Paleozoic sedimentary rocks with Vp 6.1 km/s and Vs 3.4 km/s. The corresponding Vp/Vs ratios are 3.3333 and 1.7941 and Poisson's ratios are 0.4505 and 0.2747 for sediments and rocks respectively. In addition, common reflectors in the shallower sediments at depths of 70, 120, 185, 265, 315, 500, and 593 m (Figure 18g) are also seen in the NMO migrated seismic imaging profiles for the temporary station CUKY. Those reflectors agree to the results from the reflection/refraction survey conducted near-by the CUSSO site by the University of Kentucky (Figure 19).

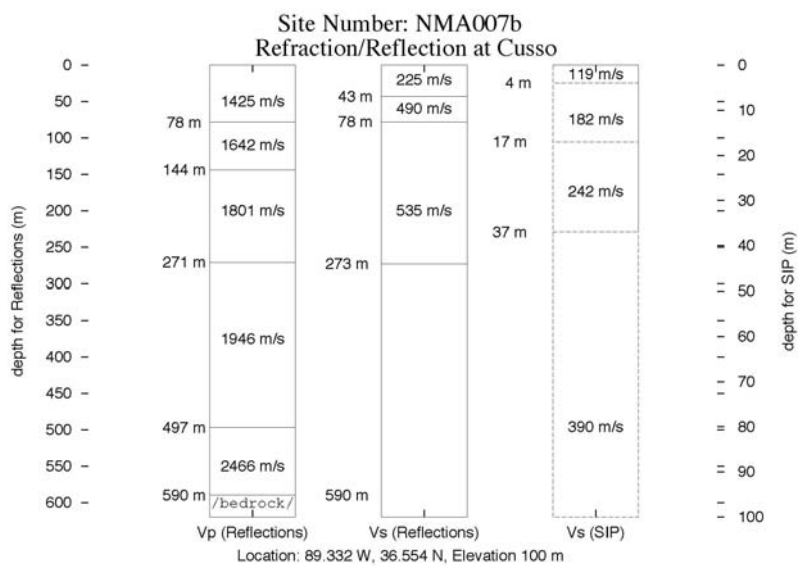

Figure 19. Velocity model for P- and S-waves resulted from the UoM/UKY reflection/refraction survey.

HICK

According to the contours of sediments derived from deep wells (Figure 15), the thickness of the unconsolidated sediments beneath the station HICK, at Hickman, Kentucky, located at 10 km east of CUSSO/CUKY, is about 584 m. Given Vp 2.0 km/s, an average shear-wave velocity of the sediments column is estimated as 0.59 km/s based on the differential travel times between the direct S and the converted Sp waves from the top of the Paleozoic sedimentary rocks for the displacement seismograms recorded on 10/18/2006 @20:59 (Figure 20a). This gives Vp/Vs 3.3401 and Poisson ratio 0.4508. The application of the pseudo-imaging method on the displacement seismograms (Figure 20b-20d) shows Vp 2.0 km/s and Vs 0.6 km/s for the unconsolidated sediments and Vp 6.0 km/s and Vs 3.4 km/s for the Paleozoic sedimentary rocks (Figure 20c). It corresponds to Vp/Vs 3.333 and Poisson ratio 0.4505 as well as Vp/Vs 1.7647 and Poisson ratio 0.2635 for the sediments and Paleozoic sedimentary rocks, respectively. NMO migrated imaging sections show strong

common reflectors associated with the geological stratigraphies at the base of unconsolidated Super group (S) and at the base of the Knox group (k). However, it seems no clear evidence of the existence of low velocity Elvins shale and the Bonneterre Formation (B) (Figure 20c). Again, shallow common reflectors are observed at depths of 70, 120, 185, 265, 310, 500 and 584 m (Figure 20c). All these results are similar to that obtained above for the station CUKY.

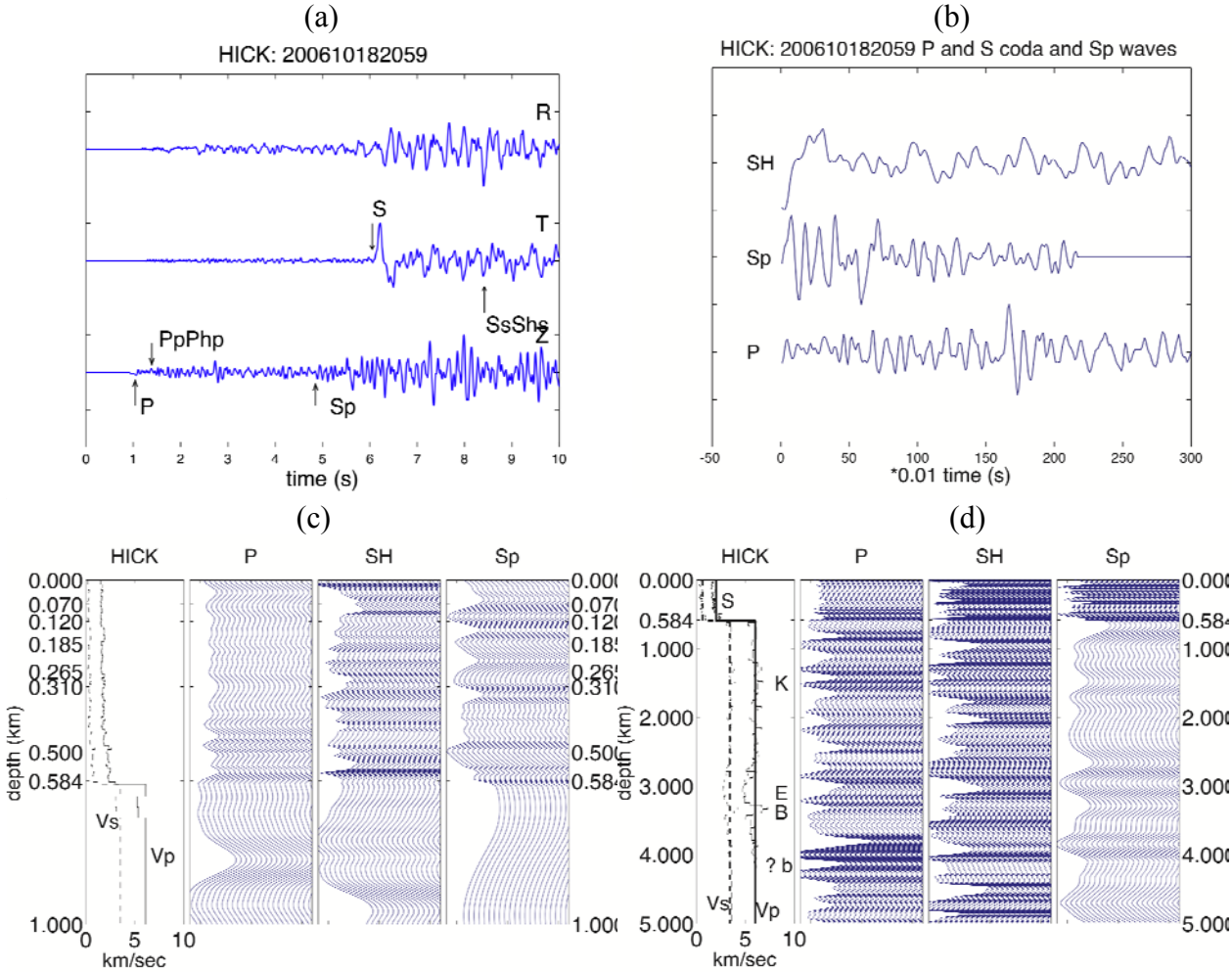

Figure 20. Pseudo-imaging profiles for station HicK (same format as Figure 18). (a) Displacement seismograms (RTZ components) recorded at HICK for Md 3.4 earthquake. Major seismic phases are annotated; (b) P (back to Sp phase) and SH coda waves, as well as Sp converted wave displacements used in this analyses. All waveforms are corrected to the negative first motions and also are normalized to their individual maximum amplitude within actual time window; (c) NMO migrated seismic section constructed by using Vp 2.0 km/s and Vs 0.6 km/s for unconsolidated sediments down to the depth 1 km. Nafe-Drake type sediments model is used to calculate the velocity for shear wave. The velocity panel (left) consists of computed Vp using CUSSO well log data and derived Vs_data for the unconsolidated sediments. A strong reflector appears consistently well correlated to the interface at depth of 584 m among all wave types. Common reflectors are seen at depths of 70, 120, 185, 265, 315, 500, and 593 m among waves, which agree to results of the shallow reflection/refraction survey (Figure 7) conducted jointly by the University of Memphis and University of Kentucky (UoM/UKY) near the deep borehole CUSSO site; (d) NMO migrated seismic section constructed by using Vp 2.0 km/s and Vs 0.6 km/s for unconsolidated sediments overlying a half space of Vp 6.0 km/s and Vs 3.4 km/s for Paleozoic rocks (thick lines in the left panel). Details of the CUSSO and the Dow Chemical/Wilson #1 well log data are shown in the thin lines. It displays common

reflectors between P and S profiles in the deeper high-velocity image sections and associates with the stratigraphy at the nearby Dow Chemical/Wilson #1 exploration well logs. This results in vp/vs 1.7647 and Poisson ratio 0.2635 in the high-velocity Paleozoic rocks, which implies not the Poisson rocks. S: Mississippi embayment Super group; K: Knox group; E: Elvins shale; B: Bonneterre formation; b: basement. Solid lines stand for P wave and dashed lines stand for S wave in the velocity panel.

Discussions

An average shear wave velocity of 0.6 km/sec for the entire unconsolidated sediment column for the region of southwestern Kentucky seems slightly lower than that found in the west part of the embayment (0.7 km/s in Langston, 2003; Chiu and Langston, 2009). Vs 0.6 km/s obtained from the pseudo-imaging profiling agrees to the results of waveform arrival observations for P and S phases shown on the CUSSO vertical array (Figure 10), S-to-Sp differential travel times shown on Figures 10, 18a & 20a, and possible S-to-SsShs phase; however, it is much higher than the direct measurements from the CUSSO logging data (~0.4 km/s; Figures 17a&17b). It casts doubt on the accuracy of the measurements of shear wave velocity from the logging data. This could be due to the improper coupling of casing with the surrounding sediments, which is necessary in the embayment environment. Additionally, unlike results reported by Moony et. al. (1983) and Ginzberg (1983), imaging profilings do not seem to correlate with the low velocity zone related to the Elvins shale and the Bonneterre Formation at depth about 2.5 to 3.5 km beneath stations CUKY (Figure 18f) and HICK (Figure 20d) in southwestern Kentucky. More studies are needed to confirm the extent of the low velocity zone in the upper Mississippi embayment.

Our observations from the CUSSO array stations confirm that the high frequency Sp waves seen on Figures 18g & 20c are converted at the interfaces corresponding to the reflectors in the loose shallower sediments and at the base of the unconsolidated sediments while relatively long-period Sp waves are converted at deeper interfaces, e.g. in the Paleozoic sedimentary rocks. This implies that multiple Sp conversions may have occurred beneath the Mississippi embayment starting at deeper interfaces. The acoustic log wells are sparse in this region; however, with the near-by well logging data and allowing minor adjustments for shear velocity, the pseudo-imaging technique can be applied to resolve an average shallow crustal velocity model beneath the station. The essential constraints for this technique are the observed travel time differences between the direct and reflected P(S) wave and between the direct S and the converting Sp phase shown on the displacement seismograms. These results demonstrate that the NMO migrated displacement imagings not only provide insight to explore wave propagation mechanisms but also verify the dependability and reliability of this technique. It is most important that this pseudo-imaging technique using displacement seismograms of natural earthquakes is a non-invasive process.

Induced ground motions from local earthquakes seem to have been significantly affected by the response of sedimentary structure to the incoming seismic waves. The characteristic site period ($T = 4H/V$), which depends on the thickness (H) and velocity (V), provides a very useful indication of the dominant period of vibration at which the most significant amplification can be expected. Amplification (modulus of the transfer function) becomes very large as resonance of the fundamental frequency ($1/T$) is met. Figure 11 clearly shows that the frequency-dependent site amplification effect due to the unconsolidated sediments in the embayment basin associates not only with earthquake magnitude but also depends substantially on the transfer modulus of the sediment column as well as on the attenuation effect through the propagating path. Therefore, velocity structure and thickness of the sediments are of intrinsic interest in the investigation of earthquake hazard analyses and environmental engineering studies.

The results of this research can be used to examine the nature and variability of high frequency site response in the range of 5-15 Hz band and to produce velocity models that can be applied to predict the low-strain seismic effects from microearthquakes in the area. Furthermore, average velocity models for the entire embayment sedimentary column can be adapted to predict the relatively low frequency response (T=3-4sec), which is important in the seismic response of large structures such as tall buildings and bridges. These models can form the core database of detailed velocity models keyed to the existing well log data and other geotechnical information. The models can be applied to the simulation of strong ground motions, inferring site effects, and earthquake source studies. The use of models in Probabilistic Seismic Hazards Assessments (PSHA) will place constraints on ground motion variability addressing uncertainty in the PSHA estimates and can also be used to correct site effects in distance attenuation studies. These direct applications of the researches will contribute to reducing losses from earthquakes within the plate interior.

Conclusions

The newly developed method using local earthquake displacement waveform data recorded on the broadband stations (Chiu and Langston, 2009) is employed to explore the velocity model in the shallow geological structures for southwestern Kentucky. This method utilizes clearly identifiable P and S reflected wave coda and transmitted Sp converted waves. The observed travel times of the reflected P and S waves as well as converted Sp waves at the base of the unconsolidated sediments in company with well logging data provide important constraints on the identification and determination of interfaces within the shallow and relative deep sediment column. NMO migrated imagings give an average Vp 2.0 km/s and Vs 0.6 km/s for the unconsolidated sediments beneath CUKY and HICK in southwestern Kentucky, upper Mississippi embayment. The results are validated by direct waveform arrival measurements between stations at both the top and the bottom of unconsolidated sediments inside the newly operative CUSSO vertical array. This results in an average Vp/Vs ratio 3.3333 and Poisson ratio 0.4505. This study finds that the unconsolidated sediments in the upper Mississippi embayment could be the Nafe-Drake type sediments. Common reflectors are also observed at depths of 70, 120, 185, 265, 310 and 500 m within unconsolidated sediments, which are comparable to the results from the shallow reflection/refraction survey conducted near the deep borehole site by a collaborative UoM/UKY project. This study demonstrates the authenticity of the technique as well. Results of Vp 6.1 km/s and Vs 3.4 km/s beneath the station CUKY as well as Vp 6.0 km/s and Vs 3.4 km/s beneath the station HICK for the Paleozoic sedimentary rocks lead to Poisson ration 0.2741 and 0.2635 respectively. These results indicate that the Paleozoic sedimentary rocks are not Poisson rocks.

This method will enable us to empirically examine the site-specific amplification of low-strain seismic waves independently from other geotechnical field methods. The use of high-frequency (5-15 Hz) and relative low frequency (3-4 sec) earthquake body waveforms can yield structure models of various resolutions, which, in turn, will elaborate upon the importance of wave reverberation effects and also can be employed to estimate site amplification for future strong ground motions due to large earthquakes in the New Madrid seismic zone. Velocity structure models can be implemented in high frequency simulations of events to characterize the corresponding seismic wave propagation and attenuation in the shallow crust of the region.

Summary

Vp and Vs models for the selected 30 sites in the upper Mississippi Embayment were studied using earthquake data and seismic reflection/refraction profiles. Although these 30 sites represent samples at only a very small portion of the embayment region, the resultant Vp and Vs models have revealed that there are very significant lateral and vertical variations of Vp and Vs structures in the post-Paleozoic sediments through out the entire embayment region. Seismic responses of such structural variations in the unconsolidated sediments are most probably responsible for the site-specific attenuation and amplification essential for a regional earthquake hazard assessment as well as for a realistic modeling of strong ground motions expected for incoming seismic waves.

Damage patterns from the 1985 Mexico City, 1988 Armenia, 1989 Loma Prieta, 1994 Northridge, 1999 Chi-Chi, 2001 Gujurat, and 2011 Christchurch earthquakes reveal that the nature, severity, and duration of strong ground shaking depend significantly on the size and location of potential earthquake sources, geometry and type of faulting of active faults, 3-D basin response, site-specific soil conditions and seismic response, and other geotechnical factors. From studies of damage patterns (e.g. Bard and Bouchon 1985, Frankel and Vidale 1992, Paolucci et al. 1992, Frankel 1993, Graves 1993), serious questions have been raised about the validity of strong ground motion predictions based on a simple 1-D simulation. For example, Frankel (1993) noted that synthetic seismograms obtained from 2-D and 3-D modeling of basins exhibited large surface waves produced by the conversion of S-waves at the edge of the basin. Boore (1999) noticed that the response spectra of strong ground motions in the Los Angeles basin might be as much as 5 to 10 times larger than expected from standard response spectra predictions for the basin based on 1-D simulations. Thus, the integration of SH- and P-wave velocity measurements, drill hole depths, seismic sections, and sonic logs from sites widely distributed over the region will produce well-constrained 3-D Vp and Vs models of the post-Paleozoic sediments throughout the entire upper Mississippi Embayment. Knowledge of the deeper sediments is critical to ground motion modeling (Anderson et al. 1996). Major impedance boundaries within the post-Paleozoic sediments, especially at shallow depth, in the upper Mississippi Embayment will have a significant impact on the amplification and linearity/nonlinearity assessment of the strong ground motions throughout the region. Therefore, a realistic assessment of strong ground motion in the embayment is possible only when comprehensive 3-D Vp and Vs models for the sedimentary basin is available. From 3-D Vp and Vs models for the sediments, the method developed for earthquake hazard maps of the Memphis area (e.g. Gomberg et al. 2003; Cramer et al., 2004) can then be applied to the entire upper Mississippi Embayment in a similar but slightly different approach as Cramer (2006).

The high-resolution 3-D Vp and Vs models for the sedimentary basin can also provide critical constraints in the initial 3-D model to produce a fine tuned 3-D crustal velocity model in a 3-D tomographic inversion. The single-event location technique using a reliably determined 3-D crustal Vp and Vs models (Chen et al., 2006) can then be applied to relocate all earthquakes in the region to produce a more reliable earthquake catalog. Geometry of the active faults can then be better imaged based on the more reliable hypocenters. Tectonic movements along the active faults can be better explored. A better understanding of the earthquake source region and active faulting are essential input for a reliable modeling of site-specific strong ground motions. A reliable local earthquake location is extremely important to allow an affective assessment of temporal and spatial variations of regional seismicity pattern that is critical for the precursory observation in the NMSZ.

Data Management

Broadband seismic data from local, regional, and teleseismic earthquakes have been recorded continuously with 100 samples/sec at all stations. The original field data have been converted to miniseed and SAC formats for initial processing. In the summer of 2012, these data will be converted to the standard SEED format and delivered to IRIS DMC for archiving. The SEG-Y formatted P- and S-wave seismic reflection/refraction profiles will be archived at the University of Kentucky and will be available to the public upon request.

Acknowledgements

This project is supported partially by the Center for Earthquake Research and Information, the University of Memphis and by the USGS NEHRP projects G09AP00096 (University of Memphis) and (University of Kentucky) G09AP000126. Logistic supports from many land owners at Arkansas, Missouri, Tennessee and Kentucky to allow the lengthy deployment of broadband stations on their properties are highly appreciated. These land owners from each state include (1) Kentudky: Ned Kendall, David Howertow, Lisa and Roger Sims. William Bottoms, Gene Hoffmeter, Juanite M and Ronnie Lawson, Joe L. Young, Lynn Dunn, Tevesh Waggonier, Rodney Martin, Michael and Marty Wallace, Danny Thurston, Charles E. Williams, Rex Gilbert, and Justus Willet; (2) Tennessee: Melroy Milbroth, J.R. and Wick Robinson, Ronald Plunk. Henry Flowers, and James E. Barnes, Steve Perkins, Danny Hipper, and Scott D. Hanley; (3) Arkansas: Robert McPherson, and Glen R. Miller; (4) Missouri: Joe Bader, Gary Carl, and Victor Rhonda Roth.

Software packages GMT (Generic Mapping Tool) (Wessel and Smith, 1998), SAC (Seismic Analysis Code) (Goldstein and Minner, 1996), and MATLAB were used in this study and are gratefully acknowledged. The Seismic Analysis Code (Goldstein *et. al*., 1996) was used for much of data processing, analyses, and preparing figures. Seismic data were obtained from the CERI Seismic Data Archive.

Attachment A– Site Locations for Seismic Profiles FY09-11

Table A

Site Name	Location	Elevation (ft)	Date
Arlington	N36°48.431' / W89°05.794'	318' (96.93 m)	7/15/10
Arlington 2	N36°48.197' / W89°01.427'	365' (111.25 m)	7/15/10
Fancy Farm West	N36°49.320' / W88°51.877'	392' (119.48 m)	7/16/10
Milburn	N36°47.136' / W88°54.896'	388' (118.26 m)	7/16/10
Fancy Farm East	N36°49.348' / W88°45.862'	507' (154.53 m)	7/22/10
Hickory	N36°47.342' / W88°38.551'	434' (132.28 m)	7/23/10
West Plains	N36°48.258' / W88°31.091'	372' (113.38 m)	3/17/11
West Plain Quad(2)	N36°49.222' / W88°37.262'	454' (138.38 m)	3/17/11
Bandana Quad	N37°11.888' / W88°58.870'	338' (103.02 m)	3/18/11
Olmsted Quad	N37°10.888' / W89°01.444'	328' (99.97 m)	3/18/11
Lacenter Quad	N37°04.808' / W88°58.196'	349' (106.37 m)	3/18/11
Wyatt Quad	N36°59.101' / 89°08.670'	Previous Study Data	
Grand Rivers Quad(3)	N37°02.005' / W88°12.649'	345' (105.16 m)	6/8/11
Calvert City Quad(3)	N37°01.073' / W88°19.528'	342' (104.24 m)	6/8/11
East Paducah(2)	N37°02.340' / W88°30.188'	348' (106.07 m)	6/9/11
Little Cyprus	N37°02.747' / W88°24.936'	340' (103.60 m)	6/9/11
Calvert City (4)	N37°03.318' / W88°21.234'	344' (104.85 m)	6/9/11
Barlow	N37°03.692' / W88°05.901'	313' (95.40 m)	6/9/11
Paducah West	N37°05.623' / W88°40.189'	367' (111.86 m)	6/10/11
Joppa	N37°10.281' / W88°48.999'	320' (97.54 m)	6/10/11
Barlow (2)	N37°05.909' / W89°05.867'	316' (96.32 m)	6/22/11
Heath (2)	N37°04.086' / W88°51.667'	441' (134.42 m)	6/22/11
Oak Level	N36°47.719' / W88°27.462'	384' (117.04 m)	6/23/11
Oak Level (2)	N36°47.644' / W88°24.811'	429' (130.76 m)	6/23/11
Hardin	N36°46.352' / W88°16.532'	416' (126.80 m)	6/23/11
Fairdealing	N36°48.002' / W88°10.885'	371' (113.08 m)	6/23/11
Fenton	N36°46.514' / W88°06.287'	374' (113.99 m)	6/23/11
Cache	N37°05.549' / W89°15.809'	321' (97.84 m)	7/5/11
Morley	N37°05.856' / W89°31.643'	329' (100.28 m)	7/6/11
Sturdivant	N37°05.913' / W90°01.783'	364' (110.95 m)	7/6/11
Bell City	N37°05.115' / W89°46.542'	333' (101.50 m)	7/6/11
Anniston	N36°47.512' / W89°19.150'	311' (94.79 m)	7/6/11
South Sikeston	N36°47.319' / W89°36.502'	293' (89.31 m)	7/6/11
Rombauer	N36°48.199' / W90°18.978'	325' (99.06 m)	7/7/11
Dexter	N36°47.104' / W89°56.846'	311' (94.79 m)	7/7/11

References

Anderson, J.G., Y. Lee, Y. Zeng, and S. Day, (1996). Control of strong motion by the upper 30 meters. *BSSA*. 86, 1749-1759.

Andrews, M.C., W.D. Mooney, and R.P. Meyer, (1985). The relocation of microseismity in the northern Mississippi embayment, *JGR*. 90, 10223-10236.

Bard, P.-Y. and M. Bouchon, (1985). The seismic response of sediment-filled valleys. Part II. The case of incident P and SV waves. *BSSA*. 70, 1921-1941.

Bauer, R.A., (2004), Final technical report: central U.S. shear wave velocity database with accompanying geological/geotechnical information of nonlithified geologic materialsm external grand award number 04-HQ-GR-0074, CUSEC State Geologists, p 29.

Bodin, P. and S. Horton, (1999). Broadband microtremor observation of basin resonance in the Mississippi embayment, Central U.S. GRL., 26, 903-906.

Bodin, P., K. Smith, S. Horton, and H. Hwang, (2001). Microtreemor observations of deep sediment resonance in metropolitan Memphis, Tennessee, Eng. Geol., 62, 159-168.

Boore, D.M., (1999). Basin waves on a seafloor recording of the 1990 Upland, California, earthquake; Implications for ground motions from a larger earthquake. *BSSA*. 89, 317-324.

Carver, D. and S.H. Hartzell, (1996). Earthquake site response in Santa Cruz, California. *BSSA*, 86, 55-65.

Catchings, R.D. (1999). Regional V_P, V_S, V_P/V_S and Poisson's ratios across earthquake source zones from Memphis, TN, to St. Louis, MO, BSSA., 89, 1591-1605.

Chen, H., J.M. Chiu, J. Pujol, K.H. Kim, K.C. Chen, B.S. Huang, Y.H. Yeh, and S.C. Chiu, (2006), A simple algorithm for local earthquake location using 3-dimensional Vp and Vs models – test examples in the central USA and Taiwan regions, Bull. Seismo. Soc. Am., 96(1), 288-305.

Chen, K.C., J.M. Chiu, and Y.T. Yang, (1994). Q_p-Q_s relation in the sedimentary basin of the upper Mississippi embayment using converted phases, *BSSA*. 84, 1861-1868.

Chen, K.C., J.M. Chiu, and Y.T. Yang, (1996). Shear-wave velocity of the sedimentary basin in the Upper Mississippi embayment using *S*-to-*P* converted waves, *BSSA*. 86, 848-856.

Chiu, J.M., A.C. Johnston and Y.T. Yang, (1992). Imaging the active faults of the central New Madrid seismic zone using PANDA array data. *Seismo. Res. Lett.*, 63, 375-393.

Chiu, J.M., C. Obikili, E. Woolery, and Z. Wang, (2011). High-resolution Vp and Vs structure of the Post-Paleozoic sediments in western Kentucky and northwestern Tennessee of upper Mississippi Embayment, presented April 2011 in the Annual SSA meeting, Memphis.

Chiu, S.C. and C.A. Langston, (2009). Reflection and transmission imaging of the upper crust using local earthquake seismograms, BSSA., 99(5), 3039–3054.

Chiu, S.C. and C.A. Langston (2011). Waveform Inversion for Near-surface Structure in the New Madrid Seismic Zone. BSSA., 101(1), 93-108.

Chiu S.C., J.M. Chiu, C.A. Langston, Z. Wang, and E Woolery (2011). Two-Dimensional Velocity Structure in the Upper Mississippi Embayment Using Passive Seismic Waveforms, Present at the SSA meeting in Memphis, TN, April 13-15, 2011.

Chiu S.C., J.M. Chiu, C.A. Langston, Z. Wang, and E Woolery (2012). Imaging the Shallow Crustal Structure in Southwestern Kentucky by using Microearthquake Waveforms, to be submitted to *Bull. Seism. Soc. Am*

Cramer, C.H., (2001). Preliminary site amplification investigation for the Memphis-Shelby county area of Tennessee using Vs30, *Seismo. Res. Lett.*, 72(1), 127.

Cramer, C.H., J.S. Gomberg, E.S. Schweig, B.A. Waldron, and K. Tucker, (2004). The Memphis, Shelby County, Tennessess, Seismic Hazard Maps, *U.S. Geol. Surv. Open-File Report* 04-1294.

Cramer, C.H., (2006), Quantifyinf the uncertainty in site amplification modeling and its effects on site-specific seismic hazard estimation in the upper Mississippi Embayment and adjacent areas, *BSSA*, 96(6), 2008-2020.

Dart, R.L., (1992). Catalog of pre-Cretaceous geologic drill-hole data from the UpperMississippi Embayment: A revision and update of Open-File Report 90-260, *USGS, Open-File Report, 92-685*, 253 pp.

Dorman, J., and R. Smalley, (1994). Low-frequency seismic surface waves in the Upper Mississippi Embayment, *SRL,* 65, 137-148.

Frankel, A., (1993). Three-dimensional simulations of ground motions in the San Bernardino Valley, California, for hypothetical earthquakes from a Loma Prieta aftershock, *BSSA*. 82, 2045-2074.

Frankel, A. and J. Vidale, (1992). A three-dimensional simulation of seismic waves in the Santa Clara Valley, California, from a Loma Prieta aftershock. *BSSA*., 83, 2045-2074.

Frankel, A., D. Carver, E. Cranswick, T. Bice, R. Sell, and S. Hanson, (2001). Observations of basin ground motions from a dense seismic array in San Jose, California, *BSSA*, 91(1), 1-12.

Gao, F.C., (1999). High-resolution 3-D sedimentary basin and upper crustal structures from 3-D inversion of PANADA data, M.S. thesis, The University of Memphis.

Gomberg, et al. (2003). Lithology and shear-wave velocity in Memphis, Tennessee, *BSSA*, 93(3), 986-997.

Graves, R.W., (1993). Modeling three-dimensional site response effects in the Marina District Basin, San Francisco, California. *BSSA*. 83, 1242-1263.

Ginzberg. A. W. D. Mooney, A. W. Walter, W. J. Lutter, and J. H. Healy., (1983). Deep structure of nothern Mississippi embayment, *Am. Assoc. Petrol. Geol.* 67, 2031 – 2046.

Goldstein, P., and L. Minner, (1996). SAC2000: Seismic signal processing and analysis tools for the 21th century, *Seis. Res. Lett*., 67, 39.

Johnston, A.C., (1982). A major earthquake zone on the Mississippi. *Scientific. Amer.,* 246, 60-68.

Johnston, A.C. and E.S. Schweig (1996). The enigma of the New Madrid Earthquakes of 1811-1812, Ann. Rev. Earth Planet. Sci., 24, pp339 - 384

Kelson, K.I., G.D. Simpson, R.B.V. Arsdale, C.C. Haraden, and W.R. Lettis, (1996). Multiple Holocene earthquakes along the Reelfoot fault, central New Madrid seismic zone, J. Geophys. Res., 202, 6151-6170.

Langston, C.A., (2003). Local earthquake wave propagation through Mississippi embayment sediments, Part II: Influence of local site velocity structure on Qp-Qs determination, BSSA., 93, 2685 - 2702.

Langston C.A., S. C. Chiu, Z. Lawrence, P. Bodin and S. Horton, (2009). Array observations of microseismic noise and the nature of H/V in the Mississippi embayment, BSSA., 99(5), 2893–2911.

Liu, H.P., Y. Hu, J. Dorman, T.S. Chang, and J.M. Chiu, (1997). Upper Mississippi Embayment shallow seismic velocities measured in situ, *Engineering Geology,* 46, 313-330.

Mclntyre, J., Z.M. Wang, E. Woolery, and G. Steiner, (2011). Instrumentation and Installation of the Central United States Seismic Observatory, presented April 2011 in the SSA meeting, Memphis.

Mihills, R.K., (1998). A structural anlaysis of the New Madrid seismic zone from contour maps and a three-dimensional model, M.S. Thesis, The University of Memphis.

Mihills, R.K., and R.B. VanArsdale, (1999). Late Wisconsin to Holocene New Madrid seismic zone deformation, *BSSA*. 89, 1019-1024.

Mooney, W.D., M.C. Andrews, A. Ginsberg, D.A. Peters, and R.M. Hamilton, (1983). Crustal structure of the northern Mississippi embayment and a comparison with other continental rift zones, *Tectonophysics,* 94, 327-348.

Nafe, J.E.,and C.L. Drake (1957), Variation with depth in shallow and deep water marine sediments of porosity, density, and the velocities of compressional and shear waves,Geophysics, 22, 523-552.

NEHRP Recommended Provision for Seismic Regulations for New Buildings and Other Structures. FEMA-450-1/2003 Edition..

Nelson, K.D., and J. Zhang (1991). A COCORP deep seismic reflection profile across the buried Reelfoot rift, south-central United States, *Tectonophysics*, 197, 271-293.

Obikili, C., (2011), Attenuation of seismic waves in the upper Mississippi Embayment from explosion data, MS thesis, University of Memphis.

Paolucci, R., M.M. Suarez, and F.J. Sanchez-Sesma, (1992). Fast computation of SH seismic response for a class of alluvial valleys. *BSSA*. 82, 2075-2086.

Pujol, J. A. Johnston, J.M. Chiu, and Y.T. Yang, (1997). Refinement of thrust faulting models for the central New Madrid seismic zone, *Engineering Geology*, 46, 281-298.

Rimrock Geophysics, Inc., (1995). SIPT2 V-4.1 (and other programs), 56 p.

Romero, S., and G.J. Rix, (2000). Regional variations in near surface wave velocities in the greater Memphis area. *Eng. Geol.,* 61(2), 137-158.

Rix, G.J., G.L. Hebeler, and M.C. Orozco, (2002). New-surface Vs profiling in the New Madrid Seismic Zone using surface-wave methods, *Seism. Res. Lett.*, 73, 380-392.

Seismic Image Software Ltd., (1996). VISTA 7.0 Notes, 477 pp.

Stearns, R.G., (1957). Cretaceous, Paleocence, and lower Eocenc geologic history of the southern Mississippi Embayment, *Geol. Soc. Am. Bull.*, 68, 1077-1100

Street, R., E. Woolery, Z. Wang, and J. Harris (1995). A short note on shear-wave velocities and other site conditions at selected strong-motion stations in the New Madrid seismic zone. *SRL,* 66(1), 56-63.

Street, R., E. Woolery, Z. Wang, and J. Harris, (2001). NEHRP soil classifications for estimating site-dependent seismic coefficients in the central Mississippi River Valley. *Engineering Geology* 62, 123-135.

Street, R., E.W. Woolery, Z. Wang, and J.B. Harris, (2002). NEHRP soil classifications for estimating site-dependent seismic coefficients in the Mississippi embayment, Eng. Geol. 62, 123-135.

Street, R., E.W. Woolery, and J.M. Chiu, (2004). Shear-wave velocities of the post-Paleozoic sediments across the upper Mississippi Embayment, Seism. Res. Lett., 75(3), 390-405.

Tuttle, M.P., and E.S. Schweig, (1999). Towards a paleoearthquake chronology for the New Madrid seismic zone, U.S. Geol. Surv. NEHRP Ann. Rept., 17 pp.

Tuttle, M.P., J.D. Sims, K. Dyer-Williams, I.R.H. Lafferty, and E.S. Schweig, (2000). Dating of liquefaction features in the New Madrid seismic zone, U.S. Nuclear Commission, 78 pp.

Vlahovic*, G.,* C. Powell*,* and J. Chiu, (2000). Three-dimensional *P* wave velocity structure in the New Madrid seismic zone, *J. Geophys. Res.,* 105, 7999 - 8012.

Van Arsdale, R.B. and R.K. TenBrink (2000). Late Cretaceous and Cenozoic Geology of the New Madrid Seismic Zone, Bull. Seism. Soc. Am., 90, pp345-356

Wessel, P., and W.H.F. Smith, (1998). New improved version of the Generic Mapping Tools released, *Eos Trans*. AGU, 79, 579.

Williams, R.A., W.J. Stephson, A.D. Frankel, and J. Odum, (1997). Surface seismic measurements of near-surface P- and S-wave seismic velocities at earthquake recording stations, Seattle, Washington, *Earthquake Spectra*, 15(3), 20p.

Williams, R.A., W.J. Stephson, A.D. Frankel, and J.K. Odum, (2001). Using high-resolution surface seismic imaging to study earthquake site response, 2001 GSA annual meeting.

Williams, R.A., S. Wood, W.J. Stephson, J.K. Odum, M.E. Meremonte, and R. Street (2003). Surface Seismic –refraction/reflection measurement determinations of Potential Site Resonances and the Areal uniformity of NEHRP Site Class D in Memphis, Tennessee: Earthquake Spectra, v.19, 159-189.

Wills, C.J., and W. Silva, (1998). Shear-wave velocity characteristics of geologic units in California, *Earthquake Spectra*, 14(3), 533-556.

Yang, Y.T., (1992). Fault zone geometry and crustal velocity structures in the central New Madrid seismic zone using data from the PANDA seismic array, M.S. thesis, The University of Memphis, 72 pp.